RESEARCH Open Access

Check for updates

Integrating vulnerability and hazard in malaria risk mapping: the elimination context of Senegal

Camille Morlighem^{1,2*}, Chibuzor Christopher Nnanatu^{3,4}, Justice Moses K. Aheto^{3,5,6} and Catherine Linard^{1,2,7}

Abstract

Background Significant efforts over the past decades have successfully reduced the global burden of malaria. However, progress has stalled since 2015. In low-transmission settings, the traditional distribution of malaria along vector suitability gradients is shifting to a new profile, with the emergence of hotspots where the disease persists. To support elimination in this context, it is essential that malaria risk maps consider not only environmental and climatic factors, but also societal vulnerabilities, in order to identify remaining hotspots and ensure that no contributing factors are overlooked. In this paper, we present an integrated approach to malaria risk mapping based on the decomposition of malaria risk into two components: 'hazard', which refers to the potential presence of infected vectors (e.g. influenced by rainfall and temperature), and 'vulnerability', which is the predisposition of the population to the burden of malaria (e.g. related to health care access and housing conditions). We focus on Senegal, which has a heterogeneous malaria epidemiological profile, ranging from high transmission in the south-east to very low transmission in the north, and which aims to eliminate malaria by 2030.

Methods We combined data from several sources: the 2017 Demographic and Health Survey (DHS) (national coverage) and the 2020-21 Malaria Indicator Survey (MIS) (south-east regions), as well as remotely sensed, high-resolution covariate data. Using Bayesian geostatistical models, we predicted the prevalence of malaria in children under five years of age with a spatial resolution of 1 km.

Results Including vulnerability factors alongside hazard factors in the 2017 DHS data model improved the accuracy of predictive maps, achieving a median predictive R² of 0.64. Furthermore, models including only vulnerability factors outperformed those including only hazard factors. However, the models trained on the 2020-21 MIS data performed poorly, achieving a median R² of 0.13 at best for the model based on hazard factors, likely due to data collection during the dry season.

Conclusions These findings highlight the importance of integrating both vulnerability and hazard factors into predictive maps. Future work could validate this approach further using routine malaria data from health management information systems, such as DHIS2.

*Correspondence: Camille Morlighem camille.morlighem@outlook.be

Full list of author information is available at the end of the article



© The Author(s) 2025. **Open Access** This article is licensed under a Creative Commons Attribution-NonCommercial-NoDerivatives 4.0 International License, which permits any non-commercial use, sharing, distribution and reproduction in any medium or format, as long as you give appropriate credit to the original author(s) and the source, provide a link to the Creative Commons licence, and indicate if you modified the licensed material. You do not have permission under this licence to share adapted material derived from this article or parts of it. The images or other third party material in this article are included in the article's Creative Commons licence, unless indicated otherwise in a credit line to the material. If material is not included in the article's Creative Commons licence and your intended use is not permitted by statutory regulation or exceeds the permitted use, you will need to obtain permission directly from the copyright holder. To view a copy of this licence, visit http://creativecommons.org/licenses/by-nc-nd/4.0/.

Keywords Demographic and Health Surveys, Malaria, Senegal, Hazard, Vulnerability, Bayesian geostatistical modelling

Background

With the inclusion of malaria incidence reduction in the Millennium Development Goals and the establishment of the Roll Back Malaria initiative, the year 2000 marked a major turning point in the fight against malaria, and significant efforts have been made to control the disease over the past decades [1]. Between 2000 and 2015, malaria mortality fell sharply from 864,000 to 586,000 deaths globally [2] due to a combination of increased resources and improved interventions made possible by effective malaria control tools such as artemisinin-based combination therapies (ACTs) and insecticide-treated nets (ITNs) [3, 4]. The first decades of the 21st century were also marked by advances in disease risk mapping pioneered by the Malaria Atlas Project [1, 5-7], which may have contributed to this progress. However, since 2015, malaria cases and deaths have stagnated and even increased in 2020 due to the disruption of health services caused by the COVID-19 pandemic [2]. In 2023, malaria deaths were still estimated at 597,000, with over 95% occurring in Sub-Saharan Africa (SSA), predominantly caused by the Plasmodium falciparum (P. falciparum) parasite [8]. With reductions in malaria incidence of up to 50-75% in high-burden countries in recent decades [4, 9], we are now entering the next stage in the fight against malaria, towards which an increasing number of countries are moving, and some have already achieved: elimination [3, 4]. However, the profile of malaria endemicity in low-transmission settings has shifted from the typical distribution along vector suitability gradients to the emergence of hotspots and 'hotpops'-populations that sustain malaria transmission due to socio-demographic risk factors [10]—where the disease persists [9– 12]. These hotspots often coexist with areas of moderate to high malaria transmission, resulting in a heterogeneous malaria epidemiological profile that challenges the achievement of national elimination goals [13, 14].

This change in the malaria epidemiological profile and the intervention strategies, which now aim at malaria elimination [4], requires an update of the current technologies and tools used to map malaria risk. Achieving malaria elimination requires targeting malaria in the remaining hotspots and 'hotpops' and therefore incorporating (and identifying) the factors that sustain the disease in low-transmission settings, rather than focusing only on the traditional climatic and environmental factors that have historically explained disease distribution in space. Instead, the conceptual framework of [15] shows that malaria risk is the result of interactions between two key components: the hazard and the vulnerability of societies (see Fig. 1). Hazard refers to the potential

occurrence of infected vectors and therefore includes all environmental factors that influence their presence and vectorial capacity [15]. These factors, which are typically used to map malaria risk and can be easily obtained from remote sensing, mainly relate to the climatic and land use/land cover conditions that make the environment suitable for vector breeding sites, such as temperature, rainfall, relative humidity, vegetation cover, proximity to water bodies and altitude [16–19].

Yet, the population at risk is not only those who live in an environment favourable to vector-borne diseases, but also those who are most vulnerable to them. Vulnerability is defined as the predisposition of a population to the burden of malaria due to differences in exposure, susceptibility and/or resilience [15, 21, 22]. Exposure is the likelihood or frequency of contact with an infected vector [23], which may be increased at certain times (e.g. during the rainy season) or for certain livelihoods (e.g. pastoralists) [20, 24]. Susceptibility represents the propensity of individuals to be adversely affected by malaria due to biological or socio-economic factors. For example, we know that immunity, co-infections or malnutrition influence the likelihood of clinical manifestations of malaria (i.e. biological susceptibility) [15, 21], while poverty also increases people's predisposition to malaria (i.e. socioeconomic susceptibility) [15]. Finally, resilience refers to the capacity of populations to anticipate malaria by using malaria prevention tools, to cope with malaria by having easy access to health facilities, and to recover from malaria by having access to treatment [15, 20]. The importance of considering both hazard and vulnerability is even greater in the context of global changes such as urbanisation, climate change and demographic shifts. These changes will alter malaria hazard and vulnerability, thereby affecting the transmission and distribution of the disease [3].

Despite this conceptual understanding, malaria risk maps often focus on the hazard relating to the environment's suitability for vectors and rarely consider the vulnerability of society to malaria. In a recent review of malaria risk mapping [25], 88% (n=78) of studies that used covariates included hazard factors, while only 40% (n=36) included vulnerability factors (calculations based on [25]). Of those that included vulnerability, most either assessed associations between vulnerability factors and malaria risk without incorporating them into predictive mapping [9, 13, 26–38], assumed spatially uniform vulnerability [39, 40], or produced risk maps at coarse spatial resolutions (e.g. health district) [41–48]. Only a small number of studies included vulnerability factors in fine-scale (1–5 km) risk mapping [1, 49–53]. Similarly,

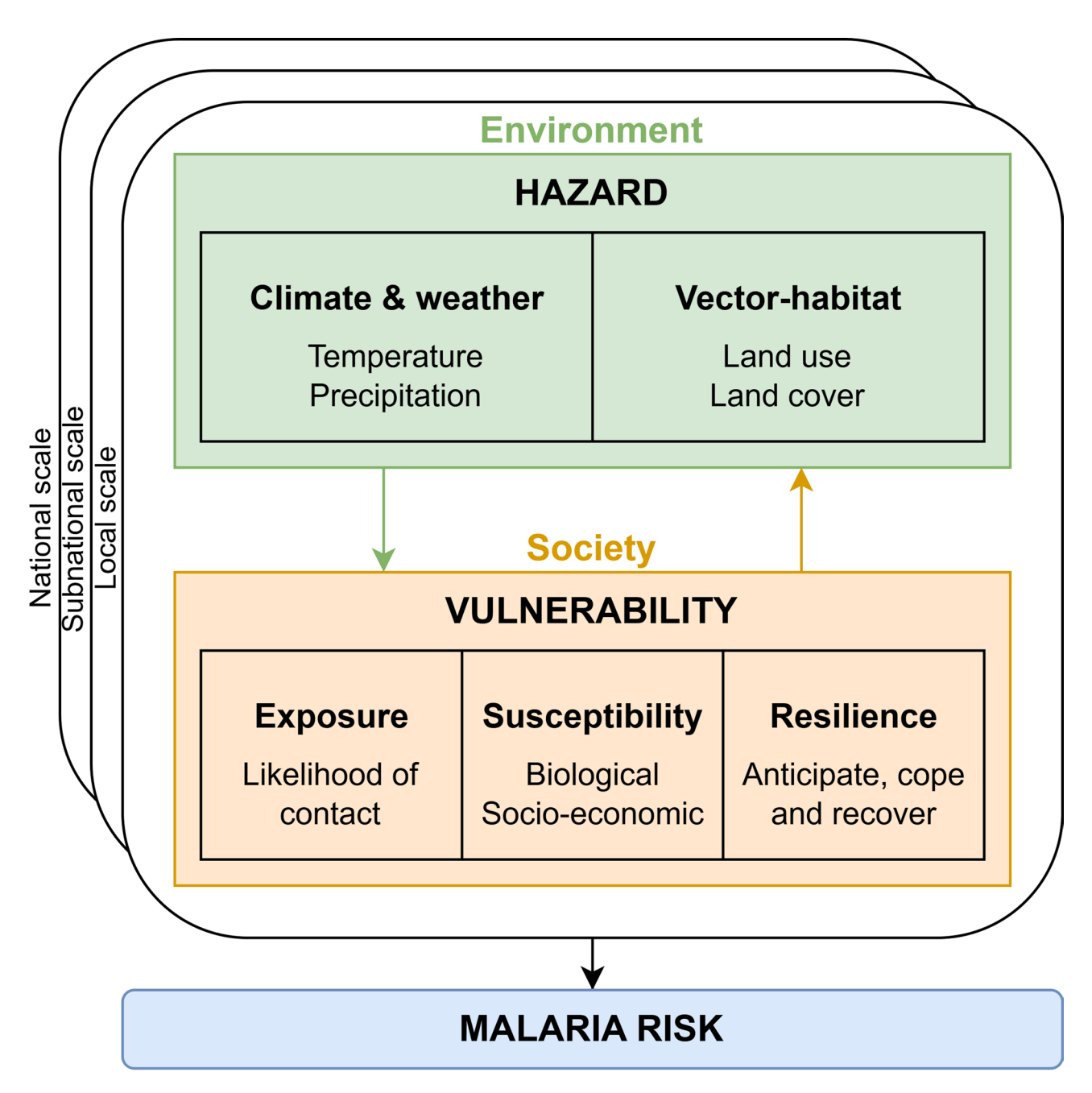


Fig. 1 The hazard-vulnerability framework of malaria risk. Adapted from [15] and [20]. This framework is based on a three-level structure. Hazard and vulnerability are the two *components* of malaria risk, each of which is composed of specific *dimensions* (e.g. climate & weather, exposure), which are quantified using measurable *factors* (e.g. temperature, wealth index)

in another review [54], 85% (n = 100) of studies that used variables beyond epidemiological ones to model or map malaria risk relied on hazard factors, while only 43% (n = 50) considered malaria vulnerability (calculations based on [54]). Across these studies, the most commonly used vulnerability factors were population density and accessibility to cities (see Table S1, Supplementary Material 1), as noted in multiple reviews [16, 25, 54]. Previous research has shown that vulnerability factors can be combined into an index to produce malaria vulnerability

maps [15]. These indices were then combined with the entomological inoculation rate through weighted aggregation approaches (e.g. weighted criteria analysis) to generate potential malaria risk maps at a resolution of 10 km [21]. In this study, we build on their work by defining additional indicators of malaria hazard and vulnerability (e.g. prevalence of anaemia, ethnicity) and using them to map malaria risk through malaria prevalence at a spatial resolution of 1 km.

In this elimination context, identifying disease hotspots in predictive maps requires high-resolution spatial data on malaria outcomes and their determinants. Two of the most commonly used sources of malaria data are routine malaria case data from health management information systems (e.g. DHIS2), which can be used to calculate malaria incidence, and household surveys, such as the Demographic and Health Surveys (DHS), which provide estimates of malaria prevalence [55]. Routine malaria data are more spatially and temporally dense because they are collected continuously through the health system [55, 56]. However, they miss individuals who do not seek care, and the actual location of infection is often unknown as cases are recorded at health facilities [55, 56]. Defining their catchment areas is challenging, even when the locations of health facilities are known [55, 56]. Although household surveys are designed to provide subnational-level estimates [57], they can still offer insights into the malaria burden at the community level, regardless of treatment-seeking behaviour [58]. Despite the spatial displacement of cluster coordinates, survey cluster locations can be used to approximate the locations of local infections. For these reasons, we used malaria prevalence estimates from household surveys to represent malaria risk in this study.

Regarding malaria determinants, previous studies of malaria risk mapping have widely used environmental variables based on freely available MODIS and Landsat satellite imagery [16, 59, 60], although these are available at low spatial resolution, or are expected to be retired in a few years (e.g. Terra satellite) [16, 59]. With advances in remote sensing and GIS technology, very high-resolution satellite imagery such as SPOT, Pléiades or QuickBird have also been used to map malaria risk at fine spatial resolution [16, 59, 61], but these are not freely available. At the same time, the Sentinel satellites of the Copernicus Programme now provide high resolution (10 m) optical imagery and appear to be a good compromise between acquisition cost and spatial resolution. In addition, largescale products based on Sentinel imagery, such as the Global Human Settlement Layer [62] and the Dynamic World land cover dataset [63], have become increasingly available in recent years. Several review studies have highlighted the missed opportunities of using Sentinel satellite imagery for malaria risk mapping and have encouraged the exploration of the potential of Sentinelderived products for this purpose [16, 64].

Among malaria-endemic countries, Senegal has seen a significant reduction in malaria cases and deaths over the past decades, thanks to the introduction of ACTs in 2006 and rapid diagnostic tests (RDTs) in 2007, and mass ITN distribution campaigns. In recent years, interventions have diversified to include seasonal malaria chemoprevention (SMC), routine ITN distribution, and active

case detection and investigation [9, 65]. Furthermore, Senegal is one of the 35 countries aiming to eliminate malaria by 2030 under the Global Technical Strategy for Malaria 2016-2030 [66]. However, since 2020, malaria cases and deaths have stagnated, particularly in the highrisk southern regions of Senegal. In 2022, the number of reported cases was more than 358,000, with 273 deaths [65]. 95% of these cases were registered in the moderate- to high-transmission zones in western (i.e. Dakar, Diourbel, Kaolack) and south-eastern Senegal (i.e. Kolda, Kédougou, Tambacounda) [65]. The other parts of Senegal has low to very low transmission, particularly in the north, with some areas classified as pre-elimination zones [65]. Previous studies have mapped malaria prevalence in Senegal for the years 2008 and 2010 [67, 68], while other research has mapped both incidence and prevalence under the assumption of temporal stationarity over extended periods (e.g. from 1990 or between 2008 and 2017) [69, 70]. While the National Malaria Control Programme has produced recent maps of malaria incidence using DHIS2 [65], the most recent MIS (2020-21) had not yet been used to model and map malaria prevalence in Senegal at the time of analysis. More detailed malaria risk maps and a better understanding of the driving factors would allow better targeting of malaria control interventions and help the country move closer to elimination.

The aim of this paper is to map malaria risk by combining different disease risk factors, covering both malaria hazard and vulnerability, to provide an integrated malaria risk mapping approach, using the elimination context of Senegal as a case study. We used data from the two most recent household surveys in Senegal which included malaria epidemiological data-the 2017 DHS and the 2020-21 MIS. Using Bayesian geostatistical models, we assessed the relationship between malaria risk factors and malaria prevalence to understand which factors sustain the disease in Senegal. We produced malaria risk maps at 1 km spatial resolution and aggregated predictions by health district after adjusting for child population counts, as policy decisions are often made at this level [17]. Furthermore, interactive web-based versions of the 1 km predictive maps were also produced to allow easy identification of hotspots for targeted malaria control. By using open-source high-resolution covariates and providing the codes that support these analyses (see [71]), the framework and methods of this study can be applied beyond Senegal.

Methods

Study area

Senegal is a West African country bordered by Mauritania, Mali, Guinea, Guinea-Bissau, Gambia and the Atlantic Ocean. Senegal is characterised by an alternation of dry and rainy seasons, with the rainy season generally

lasting from June to October [65]. Average annual rainfall, and therefore vegetation types, vary across the country from north to south, defining four ecological zones: (i) the Sahelian zone, with semi-arid grasslands and acacia savannas; (ii) the Sahelo-Sudanian zone, with flat wooded savannas; (iii) the Sudanian zone, with coexisting grasslands and woodlands; and (iv) the Sudano-Guinean zone, with dense forests and annual rainfall of over 800 mm [68]. These north-south differences in rainfall patterns also translate into differences in malaria transmission across regions (see Fig. 2). Two regional groupings, covering 52% of the population, bear almost the entire burden of malaria in the country [65]: Dakar, Diourbel and Kaloack in the west, and Kolda, Kédougou and Tambacounda in the south (see Fig. 2), also known as the KKT area. In 2022, these six regions accounted for 95% of malaria cases (30% in the first group and 65% in the second), 90% of severe cases, 84% of all malaria-related deaths, all ages combined, and 96% of deaths in children under 5 [65]. Malaria transmission remains high to moderate in these six regions, while the other eight (out of a total of 14) have low to very low transmission [65]. A new epidemiological profile is emerging in the northern regions, with hotspots of residual transmission [9, 65, 72, 73]. The main malaria parasite species is *P. falciparum*, transmitted by the main *Anopheles* (*An.*) vector species: *An. gambiae sensu stricto*, *An. arabiensis*, *An. funestus* and *An. melas* [67]. Senegal has national parks, which are areas of lower population densities, the largest being the Niokolo-Koba National Park in the KKT area (see Fig. 2).

Malaria outcome

As malaria data source, we used the two most recent household surveys conducted in Senegal that collected malaria epidemiological data: the 2017 continuous DHS and the 2020-21 MIS. The 2017 DHS was largely conducted during the rainy season (conducted between April and December), while the 2020-21 MIS was conducted during the dry season (conducted in December and January). The sampling frame of the 2017 DHS was designed to be representative at the regional level for Senegal, whereas the 2020-21 MIS collected data representative at the level of four geographical zones within Senegal (West, Centre, North and South) and at

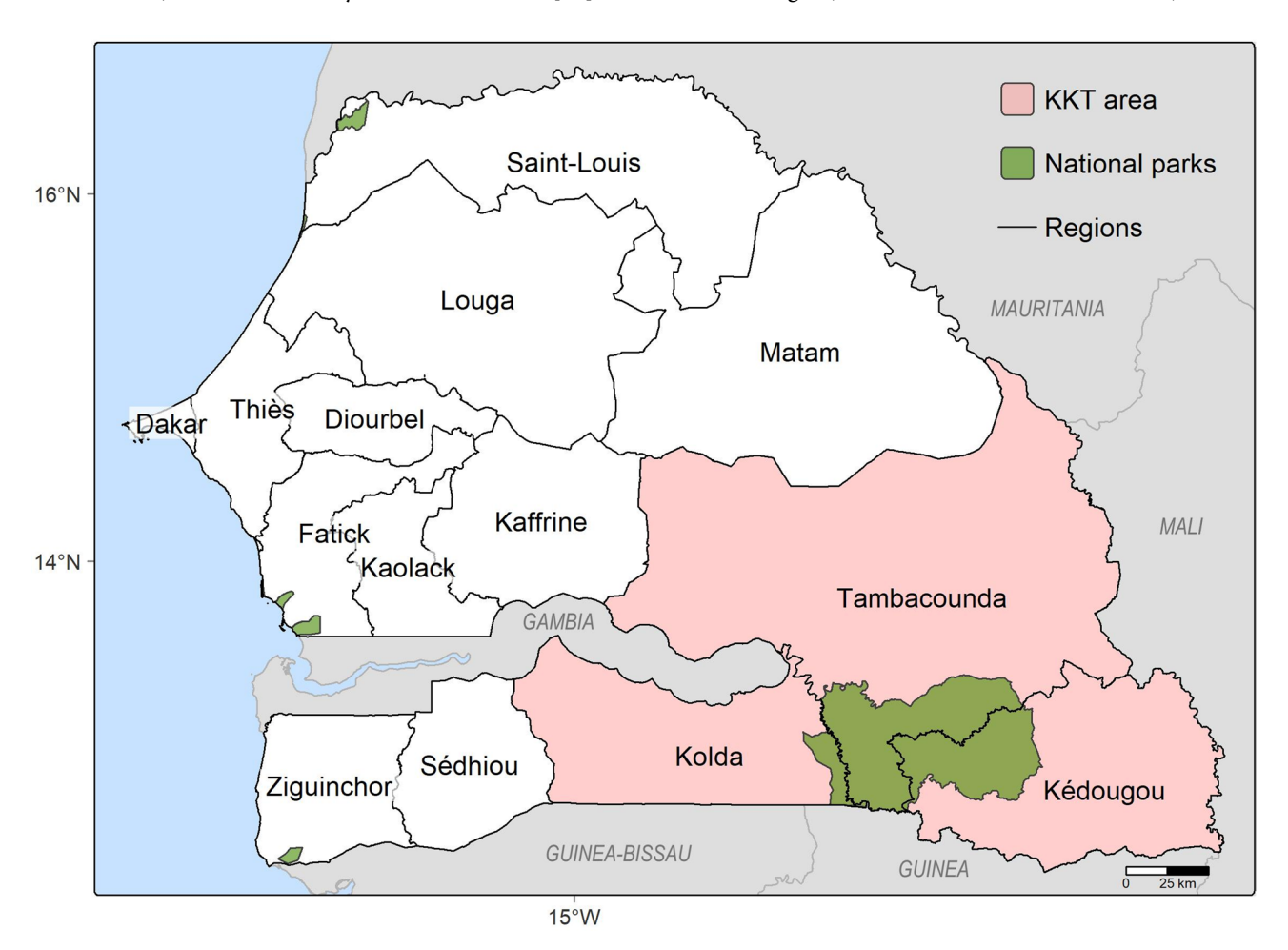


Fig. 2 Map of Senegal's 14 regions

the health district level for the southern regions, which are the areas of high malaria transmission (i.e. the KKT area; Kolda, Kédougou and Tambacounda). As a result, the sampling frame for the 2017 DHS was stratified by region and by rural/urban areas, while for the 2020-21 MIS it was stratified by geographical zone/health district and by rural/urban areas. In both surveys, primary sampling units (PSUs) or clusters were defined within each stratum using the enumeration areas of the 2013 census. A two-stage sampling procedure was used, first selecting PSUs with a probability proportional to their population size in terms of resident households, and then randomly selecting a set of 20-25 households within each PSU for a questionnaire interview [74, 75]. This resulted in 400 clusters and 8,800 households for the 2017 DHS and 207 clusters and 5,175 households for the 2020-21 MIS. In the 2020-21 MIS, only the 124 clusters in the KKT area were tested for malaria.

In the 2017 DHS, all children aged 6-59 months were tested for malaria positivity using both microscopy and RDTs, whereas in the 2020-21 MIS, malaria was only tested using RDTs. Here, we used RDT results as recommended by WHO and the Roll Back Malaria Monitoring and Evaluation Reference Group in settings where high-quality microscopy is not available, such as nonendemic settings [76, 77]. The malaria outcome used to assess malaria risk was therefore the prevalence of malaria in children aged 6-59 months, aggregated at the cluster level, i.e. the percentage of children tested who have parasite antigens detected by RDTs. RDTs detect malaria parasite antigens that can persist for several weeks after treatment [77], which is convenient in this case as the 2020-21 MIS was conducted a few months after the high-transmission season. Malaria prevalence data are geolocated using the geographic coordinates of cluster centroids, but these are randomly displaced by up to 2 km in urban areas and 5 km in rural areas (with an additional 1% offset up to 10 km) to protect the privacy of survey participants [75, 78]. This spatial displacement has been shown to strongly affect the accuracy of predictions at the intra-urban scale [79–81]. We take this into account when extracting covariates. Figure 3 shows the malaria prevalence indicator aggregated per cluster for the two surveys.

Hazard and vulnerability factors

We collected a set of environmental and socio-demographic variables covering the different dimensions of malaria hazard and vulnerability, as described in Fig. 1. First, we selected gridded covariates that were available from public repositories, with the date of collection as close as possible to that of the surveys (i.e. 2017 for DHS and 2020 for MIS). With the aim of improving the accuracy of predictive maps, as recommended in [80, 82], we attempted to maximise the level of detail in the selection of gridded covariates, so that they all have a spatial resolution of less than or equal to 1 km. In addition to these gridded covariates, several factors relating to malaria vulnerability were calculated using data from the Senegal 2017 DHS and 2020-21 MIS and aggregated at the cluster level, following instructions from the survey reports [83, 84] and more general guidance from the DHS Program [74]. We used Bayesian geostatistical models to generate continuous gridded surfaces of these DHS indicators, as described later. In the following sections, we describe the covariates used in this study, classified according to the hazard-vulnerability framework. They are listed with their characteristics and sources in Table 1 and are described in detail (e.g. spatial resolution, reference year) in Supplementary Material 2.

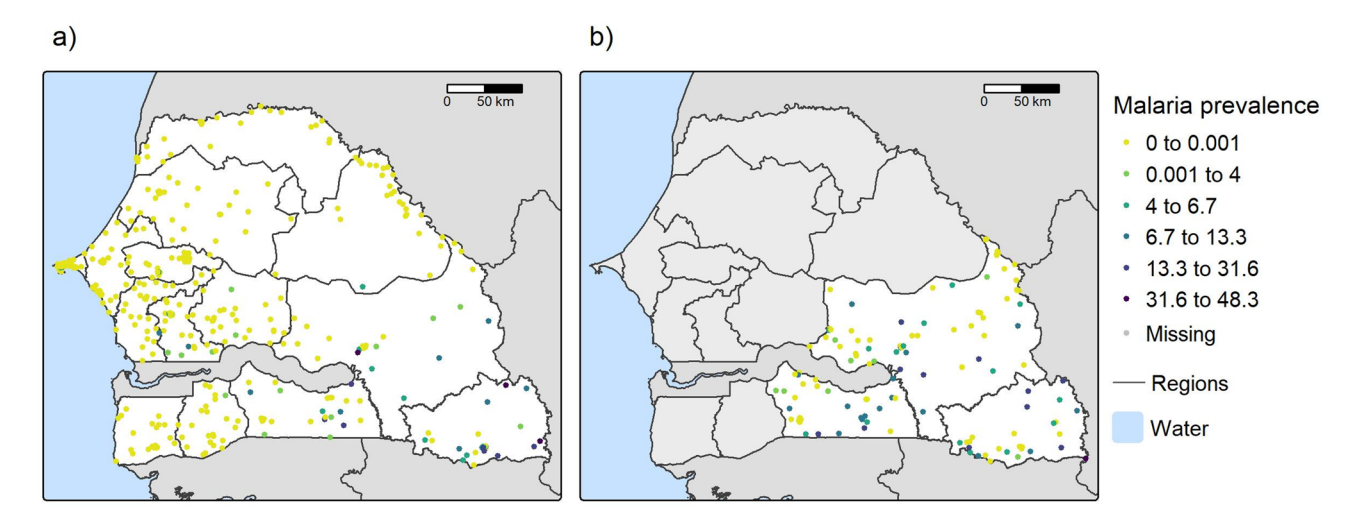


Fig. 3 Malaria prevalence in children under five per cluster of the 2017 DHS (a) and 2020-21 MIS (b). Malaria positivity was tested by rapid diagnostic tests (RDTs)

Table 1 Classification of geospatial covariates by hazard and vulnerability dimensions and their data source

Component	Dimension	Covariates	Data source
Hazard	Climate & weather	Precipitation, temperature at 2 m, potential evapotranspiration, near- surface relative humidity	CHELSA [85]
		Day land surface temperature (LST), night LST, daily LST range	MODIS [86, 87]
	Vector-habitat	Normalized difference vegetation, water and moisture indices (NDVI, NDWI, NDMI)	Computed from Sentinel-2 L1C composites of the Joint Research Centre (JRC) [88]
		Distance to water, trees, flooded vegetation, crops, grass, bare ground, shrubland	Dynamic World by Google and the World Resources Institute [63]
		Distance to human settlements	World Settlement Footprint from the German Aerospace Center [89]
		Residential built-up surface, building height	Global Human Settlement Layer from the JRC [90, 91]
		Average nighttime lights	Annual VIIRS nighttime lights v2.1 from the Earth Observation Group [92]
		Elevation	US Geological Survey [93]
Vulnerability	Exposure	Population counts	WorldPop project [94]
		Density of goat, cattle, pig, poultry, sheep	Gridded Livestock of the World v2.01 by FAO in collaboration with ILRI, the Univer- sity of Oxford and the Université Libre de Bruxelles [95]
	Susceptibility	Under-five children, pregnancies	WorldPop project [96, 97]
		Proportion of Wolof, Fula, Serer, Diola, Mandingue, Soninke, not Senegalese and other ethnic groups	ETH Zurich [98]
		Wealth index, access to basic sanitation service, malaria-related anaemia in children, stunting in children	The DHS Program
	Resilience	Distance to major roads	OpenStreetMap [99]
		Travel time to major cities, walking-only and motorized travel time to health facilities	Malaria Atlas Project [100, 101]
		Indoor residual spraying, ITN access, ITN ownership, ITN owner- ship for 2, literacy rate in women, use of intermittent preventive treatment	The DHS Program

Hazard and vulnerability dimensions are based on the conceptual framework in Fig. 1 and adapted from [15, 20]

Hazard

Climate & weather: The presence of infected vectors is highly dependent on climate and weather, with Anopheles mosquitoes thriving at temperatures between 18 and 32 °C [102] and relative humidity of at least 60% [103]. Higher relative humidity increases the life span of the vector, giving the mosquito more time to acquire and transmit the parasite [103]. In addition, high relative humidity and potential evapotranspiration usually mean high availability of surface water and soil moisture, providing suitable conditions for breeding sites [16]. Rainfall influences the presence of temporary and permanent water bodies and can also create small pools of water in which An. gambiae sensu lato prolifically breed [102, 104], although heavy rainfall can increase larval mortality through flushing and flooding [105]. We accounted for these risk factors using climate variables from CHELSA [85] and land surface temperatures (LST) from MODIS [86, 87], as LST have been widely used in previous work [16, 68].

Vector-habitat: Land use and land cover also strongly influence the presence of vectors, with water bodies, wetlands and dense vegetated areas typically providing

suitable conditions for vector breeding sites [16, 106]. Conversely, other land use categories are less favourable for vector habitat, such as bare ground (no vegetation) and built-up areas [106, 107], as vectors tend to thrive in rural rather than urban areas [106, 108]. Altitude also plays a role in shaping vector habitats, with lower elevations often indicating wetter areas and temperatures more conducive to vector development [109, 110]. To account for the suitability of the environment for vector habitat, we extracted vegetation and water indices from Sentinel-2 satellite imagery and land use/cover variables from the Dynamic World land cover dataset [63], the World Settlement Footprint [89] and the Global Human Settlement Layer [90, 91]. We also used nighttime lights [92] to indicate the presence of urban centres, and elevation was extracted from SRTM elevation data [93].

Vulnerability

Exposure: Some factors may increase the likelihood of contact with infected vectors, such as certain livelihoods. Livestock husbandry practices may increase exposure to infected vectors for pastoralists who take their herds to graze in areas that may be more suitable for the vectors.

However, some animals, such as cattle, have a protective effect against malaria because vectors prefer to feed on them rather than on humans [24, 111], while it is the opposite for other types of livestock (e.g. chickens) [111]. To account for these factors, we used gridded livestock data from the Gridded Livestock of the World project [95]. Population counts from WorldPop [94] were also included in the analysis to account for the location of potentially exposed populations.

Susceptibility: Young children and pregnant women are biologically more susceptible to clinical manifestations of malaria due to weaker immunity [24]. Genetic background can also influence susceptibility to malaria, and some ethnic groups may be genetically advantaged against malaria [24]. Co-infection with other parasitic water-borne diseases (e.g. schistosomiasis [112]) may increase the risk of malaria infection by several mechanisms, including lowering the immunological response and facilitating sporozoite infection [112]. There is increasing evidence that malnutrition also increases susceptibility to malaria [113, 114], although the relationship between malaria and malnutrition is sometimes unclear [24, 113]. Anaemia is both a risk factor and a consequence of malaria, as low levels of haemoglobin can weaken the immune system [115], increasing susceptibility to malaria, and malaria parasites cause destruction of red blood cells [24, 116]. Finally, socio-economic factors also influence malaria risk, as poverty is known to increase malaria susceptibility in several ways, including reducing access to preventive tools and influencing health-seeking behaviour [24, 117]. Several datasets were used to account for malaria susceptibility: data on children and pregnancies were extracted from WorldPop [96, 97], while ethnicity maps were obtained from the SIDE project [98]. All other susceptibility factors were derived from the DHS and MIS data: access to basic sanitation (which influences co-infection with schistosomiasis [112]), stunting in children (only available for the 2017 DHS), anaemia prevalence and a wealth index.

Resilience: Ownership and use of preventive tools such as ITNs and indoor residual spraying (IRS) have been shown to reduce malaria infections [115]. However, use of these tools may depend on beliefs, perceptions and knowledge, with women's education playing an important role in preventing malaria disease in themselves and their children [24, 115]. In addition, access to health care is a major barrier to early diagnosis and treatment of malaria [117], with people in remote and isolated areas at greater risk of severe malaria disease due to delays or lack of treatment [115, 117]. Malaria prevention indicators (i.e. ITN ownership, intermittent preventive treatment and IRS use, literacy in women) were calculated from the DHS and MIS data, while accessibility variables were extracted from travel time maps from the Malaria Atlas

Project [100, 101] and OpenStreetMap. Note that we did not use DHS indicators on the use of malaria prevention and treatment (e.g. ITN use, ACT use), following recommendations from the DHS Program [118]. These indicators are based on short recall periods, such as sleeping under an ITN the night before the survey, or treatment received in the past two weeks. Since the timing of data collection varies across locations, such short recall periods are not consistent across space, potentially introducing temporal bias into spatial analyses [118].

Processing of gridded covariates

Processing of gridded covariates included the following steps: (i) all covariates were resampled to the same 1×1 km grid to overcome differences in spatial resolution, formats, projections and spatial extents (using resample and project functions from terra R package), (ii) continuous covariates were converted to z-scores as done in [12, 119] to overcome comparability issues due to different units of measure, and (iii) covariate extraction (using exact_extract from exactextractr R package) was performed using 5 km and 2 km buffers around the geographic coordinates of rural and urban survey cluster centroids, as recommended by the DHS Program [120]. Continuous covariates were extracted using the average covariate values in the buffers, while for categorical land cover covariates, we used the average minimum distance to each class per buffer [119, 121].

Bayesian geostatistical modelling *Model structure*

In this paper, we used a Bayesian geostatistical modelling framework to model and predict the risk of malaria in children under five years of age. By treating model parameters (e.g. regression coefficients) as random variables with their own statistical properties (e.g. mean, variance), Bayesian geostatistics allow estimation of the posterior predictive distributions of the response variable, and hence makes the quantification of the uncertainty in Bayesian predictions very straightforward [122]. This ability to measure uncertainty has made them increasingly popular in recent years for modelling various health outcomes, including malaria risk [60, 68, 123–125].

Consider Y_i as the number of under-five children with a positive malaria RDT result out of N_i , the total number of children tested at cluster site s_i $(i=1,\ldots,n)$. Given the true prevalence of malaria p_i , Y_i follows a binomial distribution such that:

$$Y_i | p_i \sim Binomial(N_i, p_i)$$
 (1)

However, for the 2017 DHS, malaria positivity was tested in all regions (whereas for the 2020-21 MIS, only

south-eastern regions were tested), including northern regions with very low malaria transmission, resulting in many zero prevalence values. Therefore, for data from the 2017 DHS, we modelled Y_i using a zero-inflated binomial (ZIB) distribution, which allows zeros to be either structural zeros, where no risk of malaria has been observed, or sampling zeros, where malaria disease may be too rare an event to be detected in the sample tested:

$$Y_i \sim ZIB(N_i, p_i, \theta_i)$$
 (2)

$$Y_i|p_i, \theta_i \sim \begin{cases} 0 & \text{with probability } \theta_i \\ Binomial(N_i, p_i) & \text{with probability } 1 - \theta_i \end{cases}$$
 (3)

 θ_i , the probability of a sampling zero, is modelled as a function of the linear predictor η_i and a zero-probability hyperparameter α :

$$\theta_i = 1 - \left(\frac{\exp\left(\eta_i\right)}{1 + \exp\left(\eta_i\right)}\right)^{\alpha} \tag{4}$$

In Eqs. 1 and 2, the true prevalence p_i is linked to the linear predictor η_i through a logit link function:

$$\eta_i = \text{logit}(p_i) = \beta_0 + X_i^T \beta + u_i \tag{5}$$

$$u_i \sim \mathrm{GP}(0, \Sigma)$$
 (6)

where β_0 is the intercept, X_i is the vector of spatial covariates at site s_i , β is a vector of the corresponding unknown regression coefficients and u_i is a vector of spatially structured random effects modelled as a zero-mean Gaussian Process (GP) [126]. Spatial dependence between two observations of the GP at locations s_1 and s_2 is modelled using the Matérn covariance function Σ , defined as follows:

$$Cov(s_1, s_2) = \frac{2^{1-\nu} \sigma_u^2}{\Gamma(\nu)} (\kappa h)^{\nu} K_v(\kappa h)$$
 (7)

where h is the Euclidean distance between s_1 and s_2 , σ_u^2 is the marginal variance, $\nu>0$ controls the smoothness of the spatial process, K_v is the modified Bessel function of the second kind and $\kappa>0$ is a scale parameter controlling the range, i.e. the distance from which spatial autocorrelation is negligible. The range r is given as a function of κ such that $r=\sqrt{8\nu}/\kappa$.

Model implementation

Bayesian models were implemented within the Integrated Nested Laplace Approximation (INLA) modelling framework in conjunction with the Stochastic Partial Differential Equation (SPDE) approach [127], using the *R-INLA* package. The INLA-SPDE approach offers significant

improvements in computational complexity compared to the classical Markov chain Monte Carlo (MCMC) approaches [126]. Four different models were fitted based on different combinations of covariates (classified as in Fig. 1; Table 1): (i) the first model included no covariates (i.e. intercept-only model), (ii) the second model included all covariates related to hazard (i.e. climate & weather and vector-habitat), (iii) the third model included all covariates related to vulnerability of society (i.e. susceptibility, resilience and exposure), and (iv) the last model included all covariates, i.e. related to both hazard and vulnerability. For each model, forward stepwise variable selection was implemented directly within R-INLA using the INLAstep function (INLAutils R package), so that covariates are sequentially added to the model until adding a covariate no longer significantly reduces the Deviance Information Criterion (DIC). Further details on Bayesian geostatistical methods are provided in Supplementary Material 3.

The DIC was further used to identify the model that best fits the data among the four models tested (Intercept-only, Hazard, Vulnerability, Hazard + Vulnerability), as commonly done in the field [128]. In addition, the geostatistical models were validated using a 5-repeated 5-fold cross-validation procedure, with folds stratified to ensure that each fold contained both zero and non-zero prevalence values. The following performance metrics were calculated on the posterior mean estimates of the test sets: the mean absolute error (MAE), the root mean square error (RMSE), the coefficient of determination (R²) and the squared correlation between predicted and observed values (r²).

Predictive maps

The best-fit models for 2017 (DHS) and 2020-21 (MIS) were used to predict malaria prevalence in children under five years of age on a 1×1 km resolution grid. To support better visualisation of the predictive maps, we produced interactive web-based versions (using leaflet R package) to permit easy identification of specific highrisk communities and their names for targeted control and preventive efforts. As in previous work [61, 68], the number of infected children under five was also estimated by multiplying the predicted malaria prevalence by the high-resolution counts of children under five from WorldPop [96] (after resampling to the same spatial resolution). This represents the predicted number of children under five who would test positive for malaria if testing were conducted across the entire population of children in that age group. Population-adjusted prevalence estimates were calculated at the health district level by summing the total number of infected children under five in each health district and dividing this sum by the total number of children under five in the same health district (as estimated from the WorldPop counts).

Prior to predicting malaria prevalence, we generated predictive maps (at 1 km resolution) of the DHS indicators selected as covariates in the best-fit models using Bayesian geostatistical models. Following recommendations from [129], these models used a similar model structure as in Eq. 5, but (1) included only an intercept term and SPDE random effects (i.e. without geospatial covariates to avoid circularity issues) and (2) used a binomial likelihood for indicators representing proportions and a Gaussian likelihood for the wealth index.

Results

This study used data on 18,847 and 337 children aged 6–59 months (i.e. 0–5 years) in the 2017 DHS and 2020-21 MIS, respectively. In 2017, the observed national malaria prevalence was estimated at 0.9%, compared to 5.1% in the KKT area. In 2020-21, the observed prevalence in the KKT area was 5.3% (malaria testing only conducted in the KKT area in 2020-21). In the 2017 DHS data, 87% of clusters have zero malaria prevalence. This further demonstrates that there are different levels of endemicity across the country, with overall low malaria prevalence at the national level and the presence of higher risk areas in the south-east.

Table 2 Comparison of bayesian geostatistical models in terms of selected covariates and DIC

National models	Covariates	DIC
(2017 DHS)	Covariates	DIC
Intercept-only	/	358.76
Hazard	Potential evapotranspiration, temperature at 2 m, elevation	339.90
Vulnerability	Malaria-related anaemia in children, ITN ownership for 2, travel time to health facilities (walk), pregnancies	306.62
Hazard + Vulnerability	Malaria-related anaemia in children, ITN ownership for 2, distance to shru- bland, travel time to health facilities (walk), NDMI, proportion of Fula	<u>296.08</u>
KKT models (2020-21 MIS)	Covariates	DIC
Intercept-only	/	317.28
Hazard	Day LST, distance to grass, distance to trees	305.85
Vulnerability	Wealth index, proportion of not Senegalese	310.66
Hazard+Vulnerability	Day LST, distance to grass, distance to trees, wealth index	<u>302.30</u>

Models with the lowest Deviance Information Criterion (DIC) are underlined to indicate the best-fit models. Note that the DICs of the national and KKT models should not be compared directly, as the models were fitted to different datasets. The covariates are listed in the order in which they were selected by stepwise selection. ITN stands for insecticide-treated net, NDMI for normalized difference moisture index and LST for land surface temperature

Model selection

Model fit

The DIC [130] was used to compare different models of malaria prevalence, with the best-fit models minimising the DIC. The DIC values of the different models implemented using 2017 DHS (national level) and 2020-21 MIS (KKT area) data are shown in Table 2. For each model, a forward stepwise variable selection was implemented, so that covariates are sequentially added to the model until the addition of a covariate no longer significantly reduces the DIC.

At the national level (i.e. using 2017 DHS data), the best-fit model is obtained using both hazard and vulnerability covariates (see Table 2). The set of covariates selected by forward stepwise selection includes the following vulnerability covariates: the prevalence of malaria-related anaemia in children, the proportion of households with at least one ITN per two people, the walking time to health facilities and the proportion of Fula. The following hazard covariates were also selected: the distance to shrubland and the NDMI. Using only vulnerability covariates improved the model fit compared to using only hazard covariates, as indicated by the difference in DIC in Table 2. Similar to the national-level models, the best-fit model fitted to the 2020-21 MIS data (i.e. for the KKT area) is the one that combines both hazard and vulnerability, with the following covariates selected: day LST, distance to grass, distance to trees and wealth index (Table 2). However, in contrast to the models fitted to the 2017 DHS data, the Hazard model showed an improved fit compared to the Vulnerability model. Finally, whether for 2017 or 2020-21, all models that included hazard and/or vulnerability covariates improved model fit compared to the intercept-only models using only spatial random effects and an intercept term.

Cross-validation performance

We performed a 5-repeated 5-fold cross-validation exercise to test the predictive performance of the different models in Table 2. We used the following metrics calculated on the test sets: MAE, RMSE, R2 (coefficient of determination) and r2 (squared correlation between predicted and observed values). RMSE and MAE measure the average prediction error and are strictly positive, with smaller values indicating a better model performance. R² ranges from minus infinity to 1, with higher values indicating that the model explains more of the variance in the dependent variable [131]. r² ranges from 0 to 1 and reflects the strength of the linear relationship between the observed and predicted values (i.e. values closer to 1 indicate a stronger correlation). Estimates of these performance metrics over the cross-validated folds are given in Table 3; Fig. 4.

Table 3 Median performance metrics (MAE, RMSE, R² and r²) obtained by cross-validation

National models (2017 DHS)	MAE (%)	RMSE (%)	R ² (COD)	r² (cor- relation)
Intercept-only	1.91	4.48	0.12	0.31
Hazard	1.75	4.75	-0.09	0.30
Vulnerability	1.13	3.15	0.48	0.60
Hazard+Vulnerability	<u>1.08</u>	<u>2.86</u>	0.64	<u>0.71</u>
KKT models (2020-21 MIS)	MAE (%)	RMSE (%)	R ² (COD)	r² (cor- relation)
Intercept-only	4.82	6.33	0.09	0.13
Intercept-only Hazard	4.82 <u>4.35</u>	6.33 <u>6.31</u>	0.09 <u>0.13</u>	0.13 <u>0.20</u>
' '				

Models that minimise the RMSE and MAE and maximise the R^2 and r^2 are underlined, indicating the best model performance. The MAE, RMSE, R^2 and r^2 values were calculated on the test sets after implementing a 5-repeated 5-fold cross-validation procedure. The R^2 is the coefficient of determination (COD) and the r^2 is the square of the correlation between the observed and predicted values

At the national level (2017), the cross-validation results are consistent with the previous model DIC comparison (see Table 2). The Hazard+Vulnerability model is the best performing model with a median RMSE of 2.86, a median R² of 0.64 and a median r² (squared correlation) of 0.71 (Table 3). Furthermore, Fig. 4 shows that it is the model with the least variability in metric values across the cross-validation folds for all metrics except r². Similar to the DIC comparison (see Table 2), the Vulnerability model also outperformed the Hazard model with median

 R^2 of 0.48 and -0.09 and median squared correlation (r^2) of 0.60 and 0.30 respectively. Besides, the variability in RMSE, MAE and R^2 values across the cross-validation folds is lower for the Vulnerability model compared to the Hazard model (Fig. 4). The Intercept-only model also improved performance over the Hazard model in terms of RMSE, R^2 and r^2 (Table 3).

While there is a clear improvement in performance by using vulnerability covariates at the national level (see Fig. 4), the different models fitted to the KKT area (2020-21) do not show much difference in performance (see Fig. 4). The models performed poorly, with at best a median RMSE of 6.31, R^2 of 0.13 and r^2 of 0.20 for the Hazard model, which limits the interpretability of the estimates and results. It is also worth noting that adding covariates to the model here, whether Hazard or Vulnerability, did not improve performance as much as it did for the national-level models (see Table 3). Only the best models based on model fit and cross-validation results were retained for further analysis in this paper: i.e. the Hazard + Vulnerability model for the national level and the Hazard model for the KKT area.

Posterior estimates

Table 4 reports the posterior estimates of the parameters of the Hazard + Vulnerability model at the national level and the Hazard model in the KKT area. Since all covariates are on the same scale, as they have been transformed into z-scores, the estimated coefficients can be compared

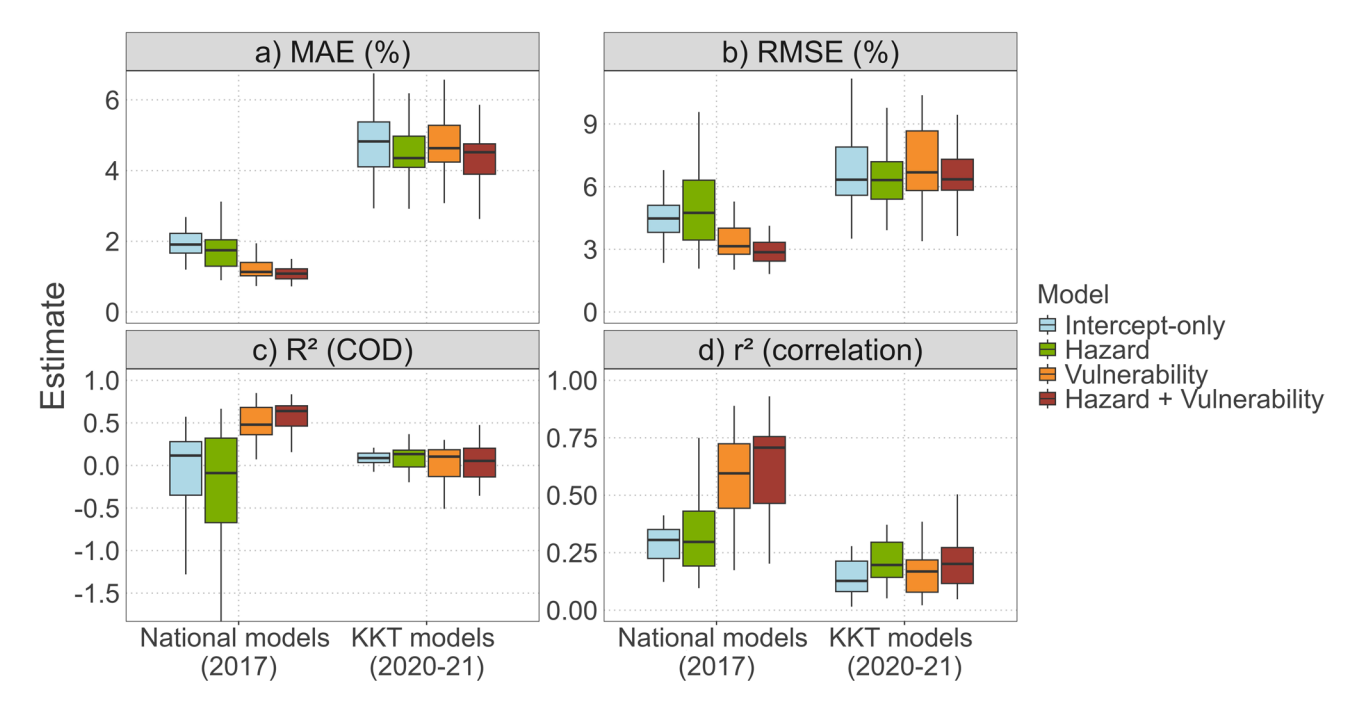


Fig. 4 Boxplot of performance metrics obtained by cross-validation. The MAE, RMSE, R^2 and r^2 values were calculated on the test sets after implementing a 5-repeated 5-fold cross-validation procedure. The R^2 is the coefficient of determination (COD) and the r^2 is the square of the correlation between the observed and predicted values. Note that outliers are not shown for the sake of readability

Table 4 Posterior estimates of bayesian geostatistical models fitted to 2017 DHS and 2020-21 MIS data

(2025) 25:1031

National model parameters (2017	Mean	2.5%	97.5%
DHS)		quantile	quantile
Intercept (eta_0)	- 5.727	- 6.810	- 4.807
Malaria-related anaemia in children	0.535	0.387	0.687
ITN ownership for 2	- 0.570	- 0.838	- 0.310
Distance to shrubland	0.688	0.257	1.144
Travel time to health facilities (walk)	0.652	0.193	1.138
NDMI	- 0.863	- 1.518	- 0.210
Proportion of Fula	0.612	- 0.006	1.261
Zero-probability parameter (α)	0.056	0.005	0.189
SD of spatially correlated variations	1.882	1.222	2.783
(σ_u)			
Range (r) (degree)	4.314 ^a	2.205	7.611
KKT model parameters (2020-21	Mean	2.5%	97.5%
MIS)		quantile	quantile
Intercept (eta_0)	- 4.428	- 5.652	- 3.267
Day LST	- 0.720	- 1.267	- 0.181
Distance to grass	1.374	0.581	2.215
Distance to trees	- 3.029	- 5.538	- 0.601
SD of spatially correlated variations	1.099	0.839	1.435
(σ_u)			
Range (r) (degree)	0.349 ^b	0.124	0.803

Posterior estimates are based on the Bayesian geostatistical models that maximised model fit and performance during model selection, i.e. the Hazard+Vulnerability model at the national level (2017) and the Hazard model for the KKT area (2020-21). Posterior estimates are reported as mean and 95% credible interval (Cl). Underlined covariates indicate significant relationships, i.e. when both the 2.5th and 97.5th percentiles of the Cl are either greater or less than zero. Note when interpreting posterior estimates that covariates were introduced into the models as z-scores. SD stands for standard deviation

 a,b These correspond to a range of 479.37 and 38.78 km respectively (1° = 111.12 km). The quantiles are obtained by taking the 95% credible intervals of the posterior estimates

to assess the relative strength of their effects on malaria prevalence. For both the national and KKT models, almost all regression coefficients are significant, as the 95% credible intervals do not include zero (see Table 4), implying strong associations with malaria prevalence.

At the national level, malaria prevalence in children aged 0-5 years had a significant positive association with child anaemia prevalence, walking time to health facilities and distance to shrubland vegetation (Table 4). ITN ownership had a protective effect against malaria, as it had a significant negative association with malaria prevalence. Malaria prevalence also decreased with increasing NDMI, suggesting that malaria prevalence is higher in areas with lower water content of vegetation. In the KKT model, malaria prevalence had a significant negative relationship with day LST and distance to trees, and a positive relationship with distance to grass. The range parameter of the national model indicates that spatial autocorrelation was present up to 479 km (1° = 111.12 km), meaning that there was a strong spatial dependence across the country, whereas this range was limited to 39 km in the KKT model (Table 4).

Predictive maps

The selected geostatistical models were used to predict malaria prevalence on a 1 km resolution grid, i.e. the Hazard + Vulnerability model at the national level (2017 DHS) and the Hazard model for the KKT area (2020-21 MIS). As the Hazard + Vulnerability model uses ITN ownership for every two people and the prevalence of malaria-related anaemia in children as covariates, this first requires the creation of interpolated surfaces of these two DHS indicators with simple Bayesian geostatistical models (with an intercept term and correlated spatial random effects). These covariate layers are not presented in detail here, but the results of the cross-validation exercise and the predicted surfaces are presented in Table S4 and Fig. S1 (see Supplementary Material 4).

Figure 5a and b show the predicted maps of malaria prevalence at 1 km spatial resolution. At the national level (Fig. 5a), there is a clear spatial trend with predicted prevalence averaging below 2% in the north of the country and western Casamance (i.e. Ziguinchor and Sédhiou) and higher prevalence areas in the KKT regions (i.e. Kolda, Kédougou, Tambacounda). Figure 6 is based on the same 2017 DHS model but focuses on the regions with very low to moderate malaria transmission (excluding Dakar, which is shown in Fig. S2, Supplementary Material 4), which allows the identification of hotspots where malaria persists, and which can facilitate elimination (see Fig. S3, Supplementary Material 4, for a zoom on the regions individually).

In the KKT area, high-risk areas are located along the borders with neighbouring countries, particularly Mali and Guinea, for both 2017 (Fig. 5a) and 2020-21 (Fig. 5b). In 2017, there is also a large hotspot overlapping with the Niokolo-Koba National Park (Fig. 5a), although associated uncertainty estimates are high (Fig. 7). Apart from the KKT area, the highest risk areas are found in Dakar-Centre (see Fig. S2, Supplementary Material 4) and in some spots in Ziguinchor and Sédhiou (Figs. 5a and 6a). However, the uncertainty maps (Fig. 7) show that these are the areas with the highest standard deviation in predicted prevalence, indicating lower confidence in the predictions in these areas. Urban hotspots can be found in several cities, including Dakar (Keur Massar, Pikine and Rufisque) (Fig. S2), Touba, Kaolack, and Thiès (Fig. 6a).

By combining the prevalence estimates with the World-Pop counts of under-five children, it was possible to estimate the number of infected children aged 0–5 years. These were then summed at health district level (Figs. 5c and d and 6c) and divided by the total child population of the district to calculate the population-adjusted malaria prevalence (AP) per health district (Figs. 5e and f and 6d). In 2017 (i.e. based on the national-level model), the health district with the highest AP is Dakar-Centre (19.8%), followed by Saraya in Kédougou (15.1%), while

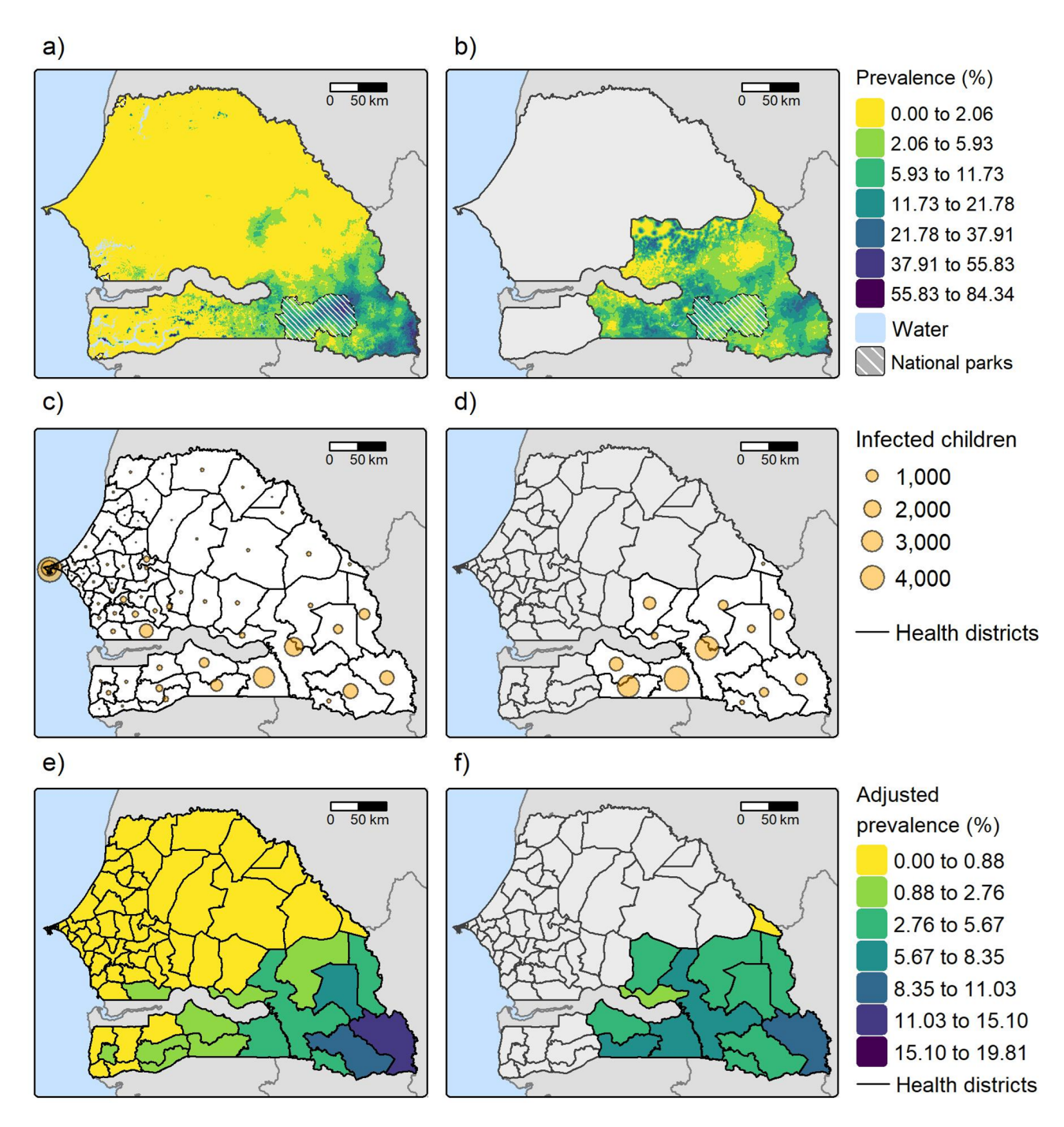


Fig. 5 Predicted malaria prevalence in children under five and number of infected children in Senegal. **a**, **b** show the posterior predicted prevalence at the national level (2017) and in the KKT area (2020-21) on a 1×1 km resolution grid, respectively. **c**, **d** show the number of infected children under five per health district, obtained by combining the predicted prevalence and child counts. **e**, **f** show population-adjusted prevalence aggregated to health district level. Posterior estimates are based on the Bayesian geostatistical models that maximised model fit and performance during model selection, i.e. the Hazard + Vulnerability model at the national level and the Hazard model for the KKT area (i.e. Kolda, Kédougou, Tambacounda)

in 2020-21 (i.e. KKT model) it is Saraya (11.0%) (see Table S5, Supplementary Material 4). Interestingly, several health districts in densely populated western Senegal (e.g. Nioro du Rip, Dakar-North) have a relatively low AP compared to districts in the KKT area (e.g. Kédougou, Saraya, Dianké Makha, Kidira), despite having a similar

or larger number of infected children (Table S5, Supplementary Material 4).

Finally, Bayesian geostatistical models can be used to quantify the uncertainty of malaria prevalence exceeding a threshold value of interest for policymakers. Figure 8 shows the probability of posterior predicted malaria

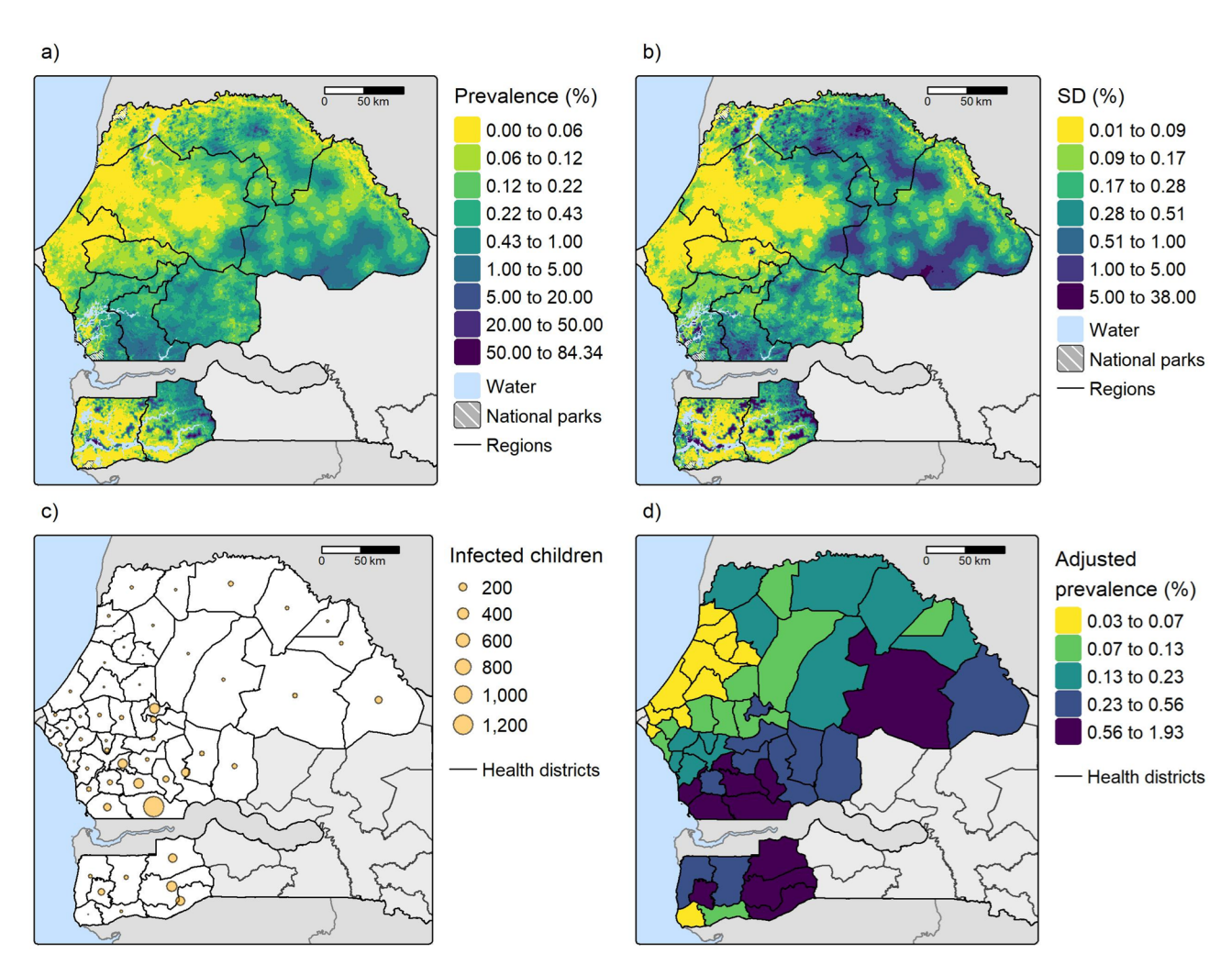


Fig. 6 Predicted malaria prevalence in children under five and number of infected children in regions of very low to moderate transmission in Senegal (excluding Dakar for visibility purposes). **a, b** show the posterior predicted prevalence and uncertainty estimates as a standard deviation (SD) on a 1×1 km resolution grid, respectively. **c** shows the number of infected children under five per health district, obtained by combining the predicted prevalence and child counts. **d** shows population-adjusted prevalence aggregated to health district level. Note that posterior estimates are based on the Hazard +Vulnerability model fitted to the complete 2017 DHS data, as for Figs. 5a, c and e, but only regions with very low to moderate malaria transmission are shown, to better highlight variation in these areas. A zoom on the Dakar region is provided in Fig. S2 (Supplementary Material 4)

prevalence exceeding 20%, with probabilities close to 0 indicating locations where prevalence is unlikely to exceed 20%, and probabilities close to 1 indicating the opposite. The interactive web-based version of Figs. 5a and b, 7 and 8 can be found in Supplementary Material 5.

Discussion

In this study, we modelled and mapped malaria risk in Senegal, a country that aims to eliminate malaria by 2030, introducing several methodological enhancements to better inform decision-making on elimination interventions. First, by combining different disease risk factors, we considered both the hazard and vulnerability components of malaria risk, avoiding the omission of factors that sustain the disease. Second, mapping malaria risk for elimination requires high-resolution data. Typically,

hazard factors rely on either free but low-resolution imagery (1 km) or expensive high-resolution imagery (<5 m) [16, 59], which limits replicability to other study areas and time periods. In this study, hazard factors were based on alternative free but high-resolution data (10 m), such as Sentinel satellite imagery and derived products to improve the accuracy of predicted maps in malaria hotspots and urban areas. We modelled malaria prevalence in children aged 0–5 years with Bayesian geostatistical models using the two most recent household surveys that collected malaria epidemiological data in Senegal: the 2017 DHS, which tested for malaria positivity in a nationally representative sample, and the 2020-21 MIS, which focused on the most endemic regions in southeastern Senegal, the so-called KKT area combining the regions of Kédougou, Kolda and Tambacounda.

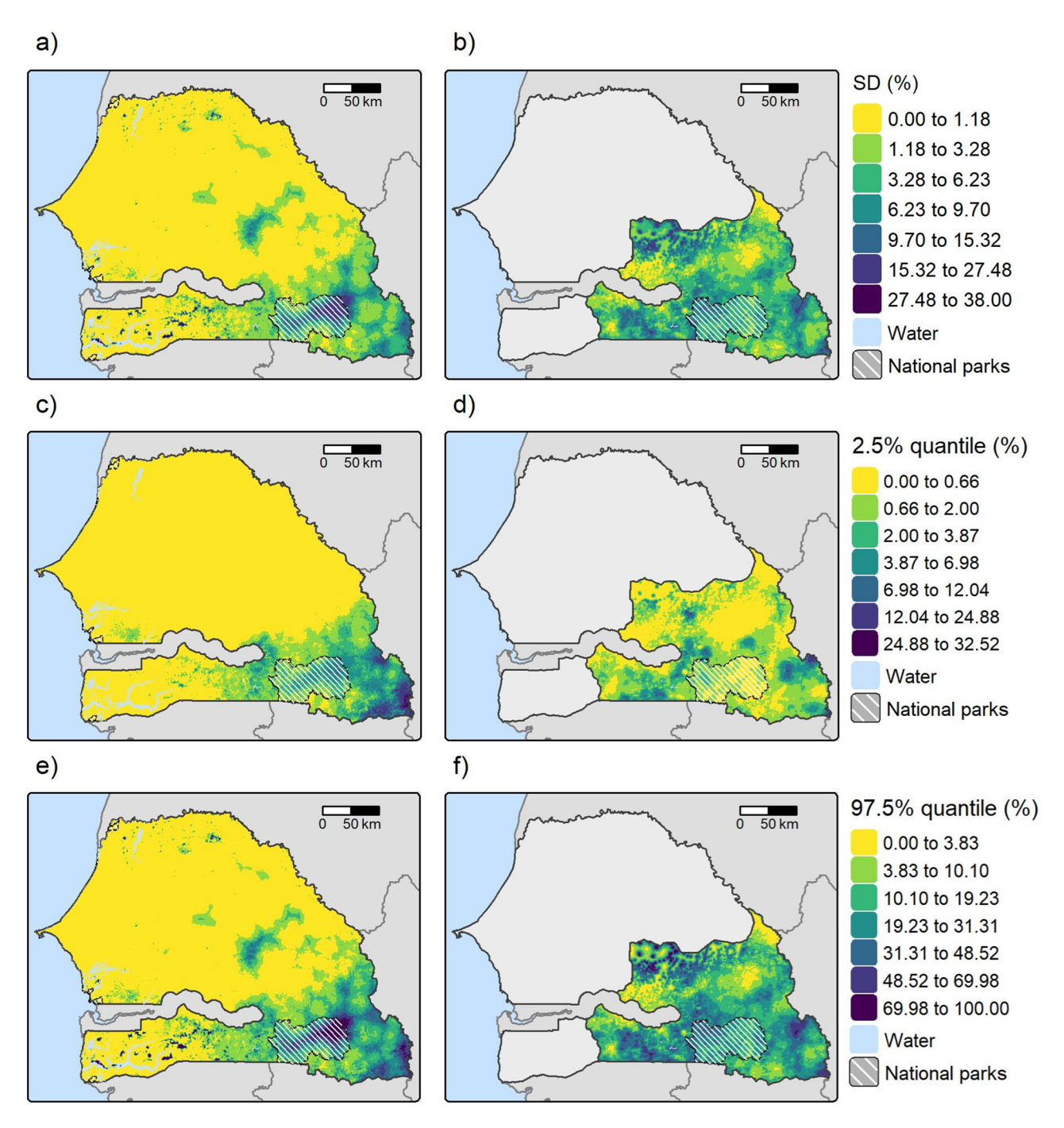


Fig. 7 Uncertainty in predicted malaria prevalence in children under five in Senegal. **a**, **b** Uncertainty is expressed as standard deviation (SD) at the national level and in the KKT area, **c**, **d** as 2.5th and **e**, **f** as 97.5th percentiles of the predicted posterior distribution of malaria prevalence. Estimates are mapped on a 1×1 km resolution grid. Posterior estimates are based on the Bayesian geostatistical models that maximised model fit and performance during model selection, i.e. the Hazard+Vulnerability model at the national level (2017) and the Hazard model for the KKT area (2020-21) (i.e. Kolda, Kédougou, Tambacounda)

Vulnerability vs. hazard

For each survey, we compared different Bayesian geostatistical models based on different combinations of hazard and vulnerability factors. We found that the bestperforming model for the 2017 DHS was the model that combined both hazard and vulnerability factors, with a median R² of 0.64, while vulnerability alone outperformed the Hazard model. However, for the 2020-21 MIS, the models performed poorly, with at best a median R² of 0.13 for the Hazard model. Overall, for the 2020-21 MIS, adding vulnerability and/or hazard covariates only slightly improved model cross-validation performance

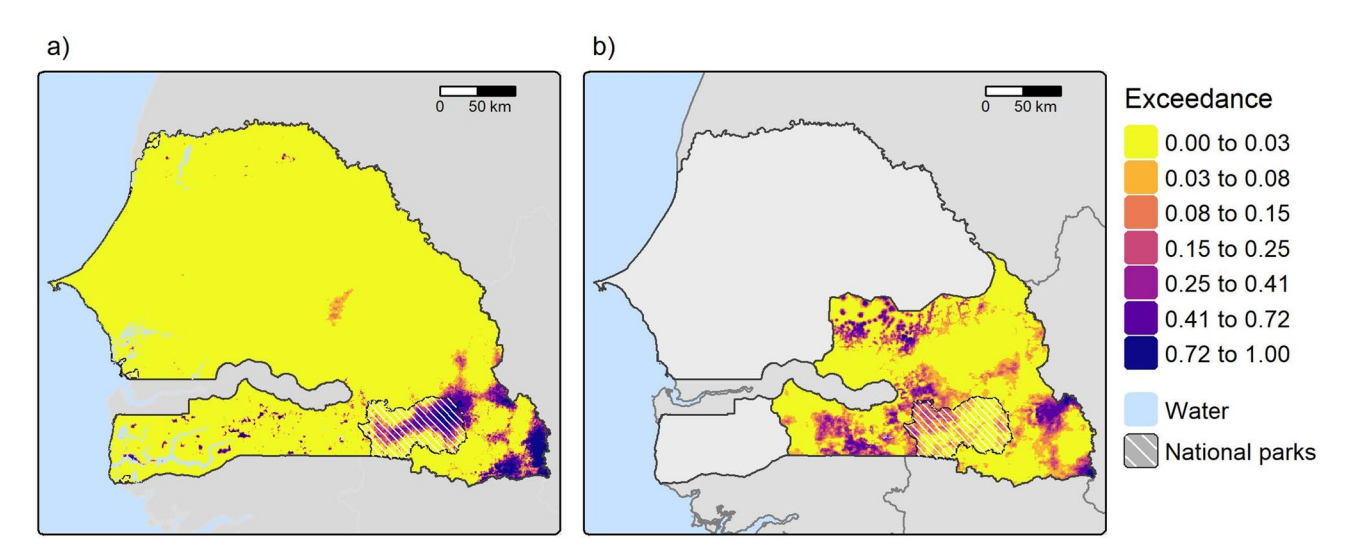


Fig. 8 Probability of posterior predicted malaria prevalence in children under five exceeding 20%. Exceedance probabilities are mapped on a 1×1 km resolution grid **a** at the national level (2017) and **b** in the KKT area (2020-21). Posterior estimates are based on the Bayesian geostatistical models that maximised model fit and performance during model selection, i.e. the Hazard+Vulnerability model at the national level (2017) and the Hazard model for the KKT area (2020-21) (i.e. Kolda, Kédougou, Tambacounda)

compared to a model using only spatial autocorrelation in the response through correlated spatial random effects. It is difficult to determine the origin of the differences in the best models fitted to the 2017 DHS and 2020-21 MIS data, as the two surveys differ in terms of year of data collection, season (i.e. the DHS was conducted mostly during the rainy season and the MIS during the dry season) and extent of the study area (i.e. the DHS is representative at the national level, while the MIS focused on the KKT area). Furthermore, the model estimates and selected covariates for the KKT area should be interpreted with caution, given the very low variance explained in the model (R² of 0.13). However, there are several possible explanations for the fact that the best model fitted to the 2020-21 MIS data included only hazard factors.

First, while there are strong socio-economic differences between urban north-west Senegal and rural south-east Senegal (i.e. the KKT area), socio-economic conditions and access to malaria prevention may be more homogeneous within the KKT area, particularly since all three regions (Kolda, Kédougou and Tambacounda) are targeted by malaria control interventions (e.g. SMC, mass ITN distribution) [65]. Consequently, vulnerability may play a lesser role in explaining malaria prevalence in this area, or the model may not accurately capture its effects. Indeed, the 2020-21 MIS data were collected in the dry season, when the number of control interventions and the percentage of households owning ITNs are lower (see Table S6, Supplementary Material 4). As a result, differences in malaria prevalence in the dry season cannot be explained by this factor alone. Furthermore, owning an ITN does not necessarily mean using it. While we did not include ITN use as a covariate, patterns of ITN use may fluctuate more significantly during the dry season, potentially influencing malaria risk more. Furthermore, malaria hotspots that emerge in the dry season may persist in an environment that remains conducive to mosquito breeding during the unfavourable season. In this context, hazard factors may be more critical: if vulnerable populations are present in areas with low vector suitability, transmission may not occur. During the rainy season, however, malaria may spread more widely due to increased environmental suitability. Therefore, differences in malaria prevalence may be partly explained by other vulnerability factors, and hotspots may be due to 'hotpops' (i.e. populations that maintain malaria transmission [10]). Lastly, differences in the importance of hazard and vulnerability factors may be due to geographic differences in transmission intensity rather than seasonality. Hazard factors may be more important in high-transmission settings (e.g. the KKT area), while vulnerability may play a greater role in areas of low transmission (e.g. where disease persists due to mobile livelihoods despite low environmental suitability). We further suggest how future work could test these hypotheses.

Key risk factors

Among the significant vulnerability factors affecting malaria, we found that having an ITN for every two people in the household had a protective effect on malaria prevalence at the national level (i.e. for the 2017 DHS). A similar relationship between ITN coverage and malaria in children and/or adolescents was observed in previous studies in Senegal [67, 68, 132] and Uganda [48]. However, the effect of prevention indicators such

as ITN coverage on malaria remains unclear in the literature, with non-protective effects of ITN coverage also reported in Ghana [60], while other studies found no significant association in Nigeria [124] and Tanzania [133]. In addition to ITN coverage, malaria prevalence was positively associated with anaemia prevalence in children—consistent with previous findings [134, 135] and with walking time to health facilities. Walking time to health facilities is a limiting factor in access to health care, with long distances and natural barriers such as rivers and mountains posing significant challenges. In Senegal, geographic accessibility to health facilities varies widely across the country, with 5% of women aged 15-49 reporting difficulty accessing health facilities due to distance, compared to 50% in Tambacounda (based on 2017 DHS estimates) [83]. Distances to health facilities are greater in the KKT area, where there are fewer roads, and heavy rains during the rainy season (i.e. the malaria transmission season) can lead to impassable flooded roads. Walking distances should be considered in relation to the status of the individual. For example, shorter distances may be more challenging for pregnant women or women with young children, who are the most vulnerable to malaria. It should be noted, however, that access to health care is multifaceted and goes beyond the geographic distance to health facilities captured in this study, as many factors influence the decision to seek care. Based on the 2017 DHS in Senegal, 53% of women aged 15-49 face at least one problem in accessing health care, with the main problems related to financial accessibility (45%), geographical accessibility (22%), reluctance to go alone (14%), and obtaining permission to seek care (7%) [83]. In a survey representative of Senegal's informal sector [136], where most workers are employed, 35% of respondents reported not seeking care when ill, with health-seeking behaviour stratified by income and type of residence. Poorer and rural households were less likely to seek care, even though the risk of malaria is higher in rural areas and poverty increases vulnerability [117]. The quality of health services can also influence health-seeking behaviour; if people are dissatisfied with the quality of health care or lack confidence in formal health services, they may turn to alternative sources, such as traditional healers or local shopkeepers, for malaria treatment [117].

In addition to vulnerability factors, we also identified important hazard factors influencing malaria prevalence in this study. At the national level (i.e. 2017 DHS), malaria prevalence was positively associated with distance to shrubland and negatively associated with the NDMI, suggesting that malaria prevalence increases as the water content of leaves and vegetation decreases. Although this sign of the relationship is not expected, such a negative correlation has also been found in [19] during the dry season in some areas of Ethiopia. Furthermore, the

areas in Senegal with the higher NDMI values are found in the regions crossed by the Casamance River and where malaria transmission is low. In the KKT area (i.e. based on 2020-21 MIS data), malaria prevalence decreased with increasing day LST. In this area, day LST (with an average of 36 °C) can largely exceed the 32 °C upper suitability threshold for *Anopheles* mosquitoes [102], explaining the negative relationship between day LST and malaria prevalence. This is consistent with previous work in Ghana [137] and Uganda [48], where malaria prevalence decreased at temperatures above 29 °C. Previous work has shown that significant environmental factors and the sign of their relationship with malaria prevalence can change depending on the season considered [137]. Mitchell et al. 2022 [138] also showed that the strength of the relationship varies according to the level of transmission.

Spatial trends in malaria risk

Other important outcomes of this study are 1 km resolution maps of posterior predicted malaria prevalence in children under five. At the national level (2017), predicted malaria prevalence shows an overall increasing gradient from northwest to southeast (see Fig. 5), with hotspots in regions of very low to moderate transmission (see Fig. 6). Several malaria hotspots have been detected in Dakar (e.g. Dakar-Centre, Rufisque, Pikine, Keur Massar) and other cities (e.g. Touba, Thiès, Kaolack), although some of these hotspots (e.g. Dakar-Centre) are associated with high uncertainty estimates indicating low confidence in the predictions. Previous studies have also identified malaria hotspots in Pikine (Dakar), as it combines optimal conditions for mosquito vectors due to the presence of an urban wetland (the Great Niaye of Pikine), alongside high population density in unplanned settlements [139–141]. Other research has reported the widespread presence of mosquito larval habitats in Touba, Kaolack and Diourbel [142, 143], as well as high entomological inoculation rates (e.g. up to 40 infectious bites per person per year in Kaolack) [142].

In recent years, the burden of malaria has increased in SSA cities [106, 121], and more studies are focusing on mapping malaria risk at the intra-urban scale [61, 81, 106, 107, 121]. Malaria burden has also increased in Dakar [65, 144] and Touba (Diourbel), particularly among children in Quranic schools (Daaras), where sleeping arrangements (e.g. sleeping outdoors or on the floor) limit ITN use [142]. Cities can also host religious gatherings such as the Grand Magal of Touba, which gathers 4 to 5 million pilgrims from Senegal and neighbouring countries annually [145, 146]. The overcrowding, lack of sanitary facilities, limited medical resources and the storage of water in open basins during this event all facilitate the transmission of malaria [143, 145, 146]. Urban areas pose

a particularly significant challenge in terms of malaria, with high population density amplifying the potential for pathogen spread [16]. Furthermore, our findings show that although malaria prevalence is generally lower in western urban areas of Senegal, the absolute number of infections can still be substantial (see Fig. 5c), sometimes surpassing that in high-prevalence rural regions in the KKT area due to the much larger urban population size.

Our predictive maps also revealed higher malaria prevalence in the KKT area, with several high-risk areas. In 2017, one such area coincides with Niokolo-Koba National Park, where environmental conditions (e.g. dense vegetation) may favour mosquito vectors and geographical access to health facilities is restricted (thereby leading to high predicted malaria prevalence in the 2017 model, see associations in Table 4). However, malaria transmission is likely to be limited in this area due to the very low density of human hosts, and it is also associated with high prediction uncertainty, likely due to the lack of nearby sampling clusters. Other high-risk areas are found at the border with neighbouring countries. The KKT area is an area of significant migration between Senegal and neighbouring countries (both immigration and emigration from and to Mali, and mainly immigration from Guinea and Guinea-Bissau) [147]. Some livelihoods may facilitate the importation of malaria. For example, longdistance truck drivers may be more exposed to mosquito vectors due to limited access to health services and accommodation, and frequent outdoor stops [148]. Traditional gold miners are also a mobile population who are frequently exposed to breeding sites through excavation activities that create stagnant bodies of water [149]. In addition, public policy on malaria often differs from country to country [150]. The lack of harmonisation of regional policies between countries is a major risk in the case of migration, as migrants become reservoirs of malaria [150]. In the context of malaria elimination, such high levels of mobility are likely to make elimination particularly challenging, as population movements can lead to continuous re-introduction of the pathogen. We encourage future research to extend our malaria risk mapping framework by incorporating indicators of weekly or seasonal mobility into the factors that influence malaria exposure (see Fig. 1). Mobile phone data (i.e. call detail records) could be used to derive metrics of human mobility in this context [151].

Limitations & future work

This study has a few limitations related to the data used, which may explain the poor performance (R² of 0.13) of the KKT models. First, the 2020-21 MIS data were collected during the dry season. This was partially mitigated by the use of RDTs that can detect malaria antigens for several weeks after parasite clearance [77]. At the same

time, this may also lead to an overestimation of prevalence in the dry season due to false positives. In addition, RDTs fail to detect low-density asymptomatic infections (less than 200 parasites/µL), which are frequent in hightransmission settings such as the KKT area [77, 152]. In addition to the timing of data collection, the quantity and quality of malaria data are limited because the 2020-21 MIS covered only 124 observation clusters (400 clusters for the 2017 DHS), and cluster coordinates are randomly displaced by up to 5 km in rural areas (2 km in urban areas) to preserve respondent anonymity. This displacement may have a greater impact on model performance at the regional level in the KKT area than at the national level. In addition, this spatial displacement could compromise the effectiveness of DHS/MIS malaria epidemiological data to be used to identify malaria hotspots and associated risk factors, particularly if the displacement distance exceeds the size of the hotspot. Another drawback of using DHS/MIS malaria prevalence data is that only children aged 0-5 years are tested in the sample, so adolescents and adults are not included in the predicted prevalence estimates. However, achieving malaria elimination may require information on prevalence in all age groups [57].

To partially account for these biases, we encourage future work to repeat these analyses using routine malaria data from the DHIS2 platform, which centralises malaria cases from health facilities in multiple countries, including Senegal. In recent years, routine malaria data have been increasingly used to model and map malaria incidence [47, 48, 153-155], including at fine spatial resolutions [11, 156-160]. Routine malaria data are reported weekly or monthly at the health facility level, providing estimates of the malaria burden over large time periods and spatial scales [55]. In the context of highly heterogeneous malaria transmission in Senegal, these data could be used to stratify malaria risk models according to seasonality and regional groupings with different levels of transmission—an approach that is difficult to implement using DHS data due to the limited number of observation clusters. Stratified risk models could then be compared to assess the heterogeneity of malaria risk factors across transmission levels and seasons. However, unlike prevalence, malaria incidence only captures those who seek care for fever (e.g. 52% of the population of Senegal in 2017 [83]), potentially missing the most vulnerable populations. Therefore, treatment-seeking behaviour needs to be accounted for in malaria incidence models.

There are also some limitations to comparing different covariates for modelling malaria prevalence. First, while we used other DHS indicators as predictors of malaria prevalence (e.g. ITN ownership, anaemia prevalence), these are observed data measured directly at the cluster level, unlike other covariates that are model outcomes

(e.g. livestock ownership). In addition, those DHS indicators are subject to the same displacement as the malaria prevalence data. This could potentially increase the importance of these covariates relative to others not extracted at the original survey cluster coordinates. We expect this bias to be insignificant, as the displacement of cluster coordinates has shown limited impact on national-level models [79], and we have accounted for displacement at covariate extraction. The accuracy of the predictive maps may be affected by the accuracy of the interpolated surfaces of DHS indicators, as errors in interpolation may propagate. This could also explain areas of high uncertainty in the predictive maps. Future research could explore how to account for uncertainty in covariate estimates within the Bayesian geostatistical models and propagate it into the uncertainty of malaria prevalence estimates.

Another limitation of this study is the temporal mismatch between the yearly averaged hazard-related covariates (e.g. temperature and land cover) and the seasonal timing of the survey. This misalignment may have weakened the observed associations between these covariates and malaria prevalence. Thanks to the high revisit frequency of MODIS and Sentinel satellites, future research could address this issue by incorporating seasonal or lagged monthly environmental covariates into spatio-temporal models that also account for the month of data collection. These adjustments could reduce uncertainty in model estimates. However, it is worth noting that persistent cloud cover in tropical regions during the rainy season limits the availability of satellite imagery [88], making it challenging to compile covariates from the wet season. Lastly, our malaria risk mapping framework could also be extended to include indicators relating to prevention and treatment behaviour (e.g. ITN use, ACT use in children with fever), although it would require addressing spatial interpolation challenges related to short survey reference periods (e.g. sleeping under an ITN the night before the survey) [118].

Strengths

This study presents an integrated malaria risk mapping framework, using a Bayesian geostatistical model to combine multiple open-access data sources, including high-resolution remotely sensed data representing hazard factors (e.g. temperature, land cover) and household survey data capturing population vulnerability (e.g. stunting in children, ITN access) and malaria prevalence. Predictive maps generated using this framework enable the identification of local malaria hotspots that may be obscured in regional or health district estimates. Such maps can therefore assist policymakers in planning targeted malaria interventions and accelerating progress towards elimination. A key advantage of Bayesian models

is their ability to quantify prediction uncertainty, which is often represented by the standard deviation or credible intervals (e.g. the 95% credible interval) of the posterior distribution of malaria prevalence estimates [122]. A higher standard deviation indicates greater uncertainty in the model's estimates [122], potentially due to sparse observations, small sample sizes, extreme covariate values or other factors [119, 161]. Uncertainty maps not only highlight areas where predictions should be treated with caution, but also inform the selection of surveillance sites [162], particularly where high prevalence coincides with high uncertainty [163]. Building on this, previous studies have demonstrated how to optimise survey locations by minimising uncertainty in current predictive maps [164]. Lastly, closely related to uncertainty estimates, our framework can also be used to map the probability that prevalence exceeds a policy-relevant threshold (i.e. exceedance probabilities) [165], which can further inform the prioritisation of interventions.

Conclusions

In this study, we present an integrated malaria risk mapping framework that combines hazard and vulnerability factors and demonstrate its application in Senegal. Using Bayesian geostatistical models, we found that integrating both hazard and vulnerability factors generally enhances malaria risk predictions, although models based on dryseason surveys underperform and gain little from added vulnerability factors. An increasing number of countries are moving to malaria elimination. In this context, the inclusion of all disease risk factors is essential to identify remaining hotspots and the factors that sustain the disease. Predictive maps generated by this integrated approach can then support decision-making for targeted interventions in hotspots, such as case investigation. Improvements in the quality of malaria data, driven by improved health management information systems, will further enhance the utility of methods such as those employed in this study. This is particularly pertinent in the context of ongoing climate change, population growth and urbanisation, all of which impact malaria vulnerability and hazard.

Abbreviations

ITN

ACT Artemisinin-based combination therapy An. AΡ Population-adjusted (malaria) prevalence **CHELSA** Climatologies at high resolution for the earth's land surface Credible interval CICOD Coefficient of determination DHS Demographic and Health Surveys DIC Deviance Information Criterion GP Gaussian process INI A Integrated Nested Laplace Approximation IPT Intermittent preventive treatment IRS Indoor residual spraying

Insecticide-treated net

JRC Joint Research Centre
KKT Kolda, Kédougou, Tambacounda
LST Land surface temperature
MAE Mean absolute error
MCMC Markov chain Monte Carlo
MIS Malaria Indicator Survey

NDMI Normalized difference moisture index NDVI Normalized difference vegetation index NDWI Normalized difference water index

P. falciparumPlasmodium falciparumPSUPrimary sampling unitRDTRapid diagnostic testRMSERoot mean square errorSDStandard deviation

SMC Seasonal malaria chemoprevention SPDE Stochastic Partial Differential Equation

SSA Sub-Saharan Africa
ZIB Zero-inflated binomial

Supplementary Information

The online version contains supplementary material available at https://doi.org/10.1186/s12879-025-11412-5.

Supplementary Material 1

Supplementary Material 2

Supplementary Material 3

Supplementary Material 4

Supplementary Material 5 Interactive web-based maps

Acknowledgements

The authors would like to thank Tidiane Ndoye (Department of Sociology, Cheikh Anta Diop University of Dakar) for his inputs on the (socio-economic) context of malaria in Senegal and for his feedback and support in interpreting the results. They also thank Sébastien Dujardin (Department of Geography, University of Namur) for his constructive suggestions and feedback on the results of this research and on the manuscript. Finally, the authors would like to thank Aminata Niang Diène (Department of Geography, Cheikh Anta Diop University of Dakar) for kindly providing the health district shapefile.

Author contributions

CM and CL led the project conception. Modelling and statistical analysis were carried out by CM with support from CCN. JMKA produced the interactive web-based maps of malaria prevalence. CM drafted the original manuscript. CL supervised the project. All authors contributed to interpretation of results, read and approved the final version of the manuscript.

Funding

Camille Morlighem is a Research Fellow of the Fonds de la Recherche Scientifique (F.R.S.-FNRS). This paper was published with the support of the University Foundation of Belgium (Fondation Universitaire de Belgique).

Data availability

2017 DHS and 2020-21 MIS data for Senegal can be accessed through the DHS Program upon registration and request at https://dhsprogram.com/data/dat aset_admin/login_main.cfm. All covariate data are open-source and links for access and download are provided in Table S3 (Supplementary Material 2). R scripts used to conduct this study are available at https://doi.org/10.6084/m9.figshare.29189567.v1 (see [71]). A simulated DHS dataset is provided at this link to demonstrate how the code works. All other data (covariates, interpolated surfaces, prediction grid) are available at the link above.

Declarations

Ethics approval and consent to participate

Not applicable.

Consent for publication

Not applicable.

Competing Interests

The authors declare no competing interests.

Author details

¹Department of Geography, University of Namur, Namur 5000, Belgium

²ILEE, University of Namur, Namur 5000, Belgium

³WorldPop, School of Geography and Environmental Science, University of Southampton, Southampton SO17 1BJ, UK

⁴Department of Statistics, Nnamdi Azikiwe University, PMB 5025, Awka, Nigeria

⁵Department of Biostatistics, School of Public Health, University of Ghana, Legon, Accra, Ghana

⁶College of Public Health, University of South Florida, Tampa, FL, USA

⁷NARILIS, University of Namur, Namur 5000, Belgium

Received: 1 July 2024 / Accepted: 21 July 2025 Published online: 18 August 2025

References

- Bhatt S, Weiss DJ, Cameron E, Bisanzio D, Mappin B, Dalrymple U, et al. The effect of malaria control on plasmodium falciparum in Africa between 2000 and 2015. Nature. 2015;526(7572):207–11. https://doi.org/10.1038/nature155
- World Health Organization. World malaria report 2023. Geneva: World Health Organization; 2023. https://cdn.who.int/media/docs/default-source/malaria/ world-malaria-reports/world-malaria-report-2023-spreadview.pdf?sfvrsn=bb 24c9f0_4.
- Strategic Advisory Group on Malaria Eradication. Malaria eradication: benefits, future scenarios and feasibility. A report of the strategic advisory group on malaria eradication. Geneva: World Health Organization; 2020. https://www.w ho.int/publications/i/item/9789240003675.
- Shretta R, Liu J, Cotter C, Cohen J, Dolenz C, Makomva K, et al. Malaria elimination and eradication. In: Holmes KK, Bertozzi S, Bloom BR, Jha P, editors.
 Major infectious diseases. 3rd ed. Washington (DC): The International Bank for Reconstruction and Development / The World Bank; 2017.
- Hay SI, Snow RW. The malaria atlas project: developing global maps of malaria risk. PLoS Med. 2006;3(12):e473. https://doi.org/10.1371/journal.pme d.0030473.
- Hay SI, Guerra CA, Gething PW, Patil AP, Tatem AJ, Noor AM, et al. A world malaria map: plasmodium falciparum endemicity in 2007. PLoS Med. 2009;6(3):e1000048. https://doi.org/10.1371/journal.pmed.1000048.
- Gething PW, Patil AP, Smith DL, Guerra CA, Elyazar IR, Johnston GL, et al. A new world malaria map: plasmodium falciparum endemicity in 2010. Malar J. 2011;10:378. https://doi.org/10.1186/1475-2875-10-378.
- World Health Organization. World malaria report 2024: addressing inequity in the global malaria response. Geneva: World Health Organization; 2024. https: //cdn.who.int/media/docs/default-source/malaria/world-malaria-reports/world-malaria-report-2024-spreadview.pdf?sfvrsn=3ccb3695_3.
- Ndiath M, Faye B, Cisse B, Ndiaye JL, Gomis JF, Dia AT, et al. Identifying malaria hotspots in Keur Soce health and demographic surveillance site in context of low transmission. Malar J. 2014;13(1):453. https://doi.org/10.1186/1475-287 5-13-453.
- Sturrock HJW, Hsiang MS, Cohen JM, Smith DL, Greenhouse B, Bousema T, et al. Targeting asymptomatic malaria infections: active surveillance in control and elimination. PLoS Med. 2013;10(6):e1001467. https://doi.org/10.1371/journal.pmed.1001467.
- Alegana VA, Atkinson PM, Lourenço C, Ruktanonchai NW, Bosco C, zu Erbach-Schoenberg E, et al. Advances in mapping malaria for elimination: fine resolution modelling of plasmodium falciparum incidence. Sci Rep. 2016;6(1):29628. https://doi.org/10.1038/srep29628.
- Sturrock HJ, Cohen JM, Keil P, Tatem AJ, Le Menach A, Ntshalintshali NE, et al. Fine-scale malaria risk mapping from routine aggregated case data. Malar J. 2014;13(1):421. https://doi.org/10.1186/1475-2875-13-421.
- Millar J, Psychas P, Abuaku B, Ahorlu C, Amratia P, Koram K, et al. Detecting local risk factors for residual malaria in Northern Ghana using bayesian model averaging. Malar J. 2018;17(1):343. https://doi.org/10.1186/s12936-018-249 1-2.

- Zhou G, Githure J, Lee MC, Zhong D, Wang X, Atieli H, et al. Malaria transmission heterogeneity in different eco-epidemiological areas of Western kenya: a region-wide observational and risk classification study for adaptive intervention planning. Malar J. 2024;23:74. https://doi.org/10.1186/s12936-024-04903-4.
- Kienberger S, Hagenlocher M. Spatial-explicit modeling of social vulnerability to malaria in East Africa. Int J Health Geogr. 2014;13(1):29. https://doi.org/10.1 186/1476-072X-13-29.
- Parselia E, Kontoes C, Tsouni A, Hadjichristodoulou C, Kioutsioukis I, Magiorkinis G, et al. Satellite Earth observation data in epidemiological modeling of malaria, dengue and West nile virus: A scoping review. Remote Sens. 2019;11(16):1862. https://doi.org/10.3390/rs11161862.
- Alegana VA, Macharia PM, Muchiri S, Mumo E, Oyugi E, Kamau A, et al. Plasmodium falciparum parasite prevalence in East Africa: Updating data for malaria stratification. PLOS Global Public Health. 2021;1(12):e0000014. https://doi.org/10.1371/journal.pgph.0000014.
- Boyce MR, Katz R, Standley CJ. Risk factors for infectious diseases in urban environments of Sub-Saharan africa: A systematic review and critical appraisal of evidence. Trop Med Infect Disease. 2019;4(4):123. https://doi.org/ 10.3390/tropicalmed4040123.
- McMahon A, Mihretie A, Ahmed AA, Lake M, Awoke W, Wimberly MC. Remote sensing of environmental risk factors for malaria in different geographic contexts. Int J Health Geogr. 2021;20(1):28. https://doi.org/10.1186/s12942-02 1-00282-0.
- Birkmann J, Cardona OD, Carreño ML, Barbat AH, Pelling M, Schneiderbauer S, et al. Framing vulnerability, risk and societal responses: the MOVE framework. Nat Hazards. 2013;67(2):193–211. https://doi.org/10.1007/s11069-013-0558-5.
- Hagenlocher M, Castro MC. Mapping malaria risk and vulnerability in the united Republic of tanzania: a Spatial explicit model. Popul Health Metrics. 2015;13(1):2. https://doi.org/10.1186/s12963-015-0036-2.
- Hagenlocher M, Delmelle E, Casas I, Kienberger S. Assessing socioeconomic vulnerability to dengue fever in cali, colombia: statistical vs expert-based modeling. Int J Health Geogr. 2013;12(1):36. https://doi.org/10.1186/1476-07 2X-12-36.
- Gibb R, Franklinos LHV, Redding DW, Jones KE. Ecosystem perspectives are needed to manage zoonotic risks in a changing climate. BMJ. 2020;371:m3389. https://doi.org/10.1136/bmj.m3389.
- Bates I, Fenton C, Gruber J, Lalloo D, Lara AM, Squire SB, et al. Vulnerability to malaria, tuberculosis, and HIV/AIDS infection and disease. Part 1: determinants operating at individual and household level. Lancet Infect Dis. 2004;4(5):267–77. https://doi.org/10.1016/S1473-3099(04)01002-3.
- Odhiambo JN, Kalinda C, Macharia PM, Snow RW, Sartorius B. Spatial and spatio-temporal methods for mapping malaria risk: a systematic review. BMJ Global Health. 2020;5(10):e002919. https://doi.org/10.1136/bmjgh-2020-0029 19
- Bennett A, Yukich J, Miller JM, Vounatsou P, Hamainza B, Ingwe MM, et al. A
 methodological framework for the improved use of routine health system
 data to evaluate National malaria control programs: evidence from Zambia.
 Popul Health Metrics. 2014;12(1):30. https://doi.org/10.1186/s12963-014-003
 0-0
- Bisanzio D, Mutuku F, LaBeaud AD, Mungai PL, Muinde J, Busaidy H, et al. Use of prospective hospital surveillance data to define Spatiotemporal heterogeneity of malaria risk in coastal Kenya. Malar J. 2015;14(1):482. https://doi.org/1 0.1186/s12936-015-1006-7.
- Bousema T, Drakeley C, Gesase S, Hashim R, Magesa S, Mosha F, et al. Identification of hot spots of malaria transmission for targeted malaria control. J Infect Dis. 2010;201(11):1764–74. https://doi.org/10.1086/652456.
- Kamuliwo M, Kirk K, Chanda E, Elbadry M, Jailos L, Weppelmann T, et al. Spatial patterns and determinants of malaria infection during pregnancy in Zambia. Trans R Soc Trop Med Hyg. 2015;109. https://doi.org/10.1093/trstmh/ trv049.
- Ndiath MM, Cisse B, Ndiaye JL, Gomis JF, Bathiery O, Dia AT, et al. Application of geographically-weighted regression analysis to assess risk factors for malaria hotspots in Keur Soce health and demographic surveillance site.
 Malar J. 2015;14(1):463. https://doi.org/10.1186/s12936-015-0976-9.
- Selemani M, Mrema S, Shamte A, Shabani J, Mahande MJ, Yeates K, et al. Spatial and space–time clustering of mortality due to malaria in rural tanzania: evidence from Ifakara and Rufiji health and demographic surveillance system sites. Malar J. 2015;14(1):369. https://doi.org/10.1186/s12936-015-0905-y.
- 32. Shaffer JG, Touré MB, Sogoba N, Doumbia SO, Gomis JF, Ndiaye M, et al. Clustering of asymptomatic plasmodium falciparum infection and the

- effectiveness of targeted malaria control measures. Malar J. 2020;19(1):33. htt ps://doi.org/10.1186/s12936-019-3063-9.
- Simon C, Moakofhi K, Mosweunyane T, Jibril HB, Nkomo B, Motlaleng M, et al. Malaria control in botswana, 2008–2012: the path towards elimination. Malar J. 2013;12(1):458. https://doi.org/10.1186/1475-2875-12-458.
- Solomon T, Loha E, Deressa W, Gari T, Lindtjørn B. Spatiotemporal clustering of malaria in southern-central ethiopia: a community-based cohort study. PLoS One. 2019;14(9):e0222986. https://doi.org/10.1371/journal.pone.022298
- Ssempiira J, Nambuusi B, Kissa J, Agaba B, Makumbi F, Kasasa S, et al. Geostatistical modelling of malaria indicator survey data to assess the effects of interventions on the geographical distribution of malaria prevalence in children less than 5 years in Uganda. PLoS One. 2017;12(4):e0174948. https:// doi.org/10.1371/journal.pone.0174948.
- Belay DB, Kifle YG, Goshu AT, Gran JM, Yewhalaw D, Duchateau L, et al. Joint bayesian modeling of time to malaria and mosquito abundance in Ethiopia. BMC Infect Dis. 2017;17(1):415. https://doi.org/10.1186/s12879-017-2496-4.
- 37. Ishengoma DS, Mmbando BP, Mandara CI, Chiduo MG, Francis F, Timiza W, et al. Trends of plasmodium falciparum prevalence in two communities of Muheza district North-eastern tanzania: correlation between parasite prevalence, malaria interventions and rainfall in the context of re-emergence of malaria after two decades of progressively declining transmission. Malar J. 2018;17(1):252. https://doi.org/10.1186/s12936-018-2395-1.
- Selemani M, Msengwa AS, Mrema S, Shamte A, Mahande MJ, Yeates K, et al. Assessing the effects of mosquito Nets on malaria mortality using a space time model: a case study of Rufiji and Ifakara health and demographic surveillance system sites in rural Tanzania. Malar J. 2016;15(1):257. https://doi. org/10.1186/s12936-016-1311-9.
- Peterson I, Borrell LN, El-Sadr W, Teklehaimanot A. A Temporal-Spatial analysis of malaria transmission in adama, Ethiopia. Am J Trop Med Hyg. 2009;81(6):944–9. https://doi.org/10.4269/ajtmh.2009.08-0662.
- Yankson R, Anto EA, Chipeta MG. Geostatistical analysis and mapping of malaria risk in children under 5 using point-referenced prevalence data in Ghana. Malar J. 2019;18(1):67. https://doi.org/10.1186/s12936-019-2709-y.
- Abellana R, Ascaso C, Aponte J, Saute F, Nhalungo D, Nhacolo A, et al. Spatioseasonal modeling of the incidence rate of malaria in Mozambique. Malar J. 2008;7(1):228. https://doi.org/10.1186/1475-2875-7-228.
- 42. Alegana VA, Atkinson PM, Wright JA, Kamwi R, Uusiku P, Katokele S, et al. Estimation of malaria incidence in Northern Namibia in 2009 using bayesian conditional-autoregressive spatial-temporal models. Spat Spatio-temporal Epidemiol. 2013;7:25–36. https://doi.org/10.1016/j.sste.2013.09.001.
- Mukonka VM, Chanda E, Kamuliwo M, Elbadry MA, Wamulume PK, Mwanza-Ingwe M, et al. Diagnostic approaches to malaria in zambia, 2009–2014. Geospat Health. 2015;10(1). https://doi.org/10.4081/gh.2015.330.
- Nyadanu SD, Pereira G, Nawumbeni DN, Adampah T. Geo-visual integration of health outcomes and risk factors using excess risk and conditioned choropleth maps: a case study of malaria incidence and sociodemographic determinants in Ghana. BMC Public Health. 2019;19(1):514. https://doi.org/10.1186/s12889-019-6816-z.
- Rouamba T, Samadoulougou S, Tinto H, Alegana VA, Kirakoya-Samadoulougou F. Bayesian Spatiotemporal modeling of routinely collected data to assess the effect of health programs in malaria incidence during pregnancy in Burkina Faso. Sci Rep. 2020;10(1):2618. https://doi.org/10.1038/s41598-02 0-58899-3
- Siraj AS, Bouma MJ, Santos-Vega M, Yeshiwondim AK, Rothman DS, Yadeta D, et al. Temperature and population density determine reservoir regions of seasonal persistence in highland malaria. Proc R Soc B. 2015;282:20151383. ht tps://doi.org/10.1098/rspb.2015.1383.
- 47. Ssempiira J, Kissa J, Nambuusi B, Kyozira C, Rutazaana D, Mukooyo E, et al. The effect of case management and vector-control interventions on space-time patterns of malaria incidence in Uganda. Malar J. 2018;17(1):162. https://doi.org/10.1186/s12936-018-2312-7.
- Ssempiira J, Kissa J, Nambuusi B, Mukooyo E, Opigo J, Makumbi F, et al. Interactions between Climatic changes and intervention effects on malaria spatio-temporal dynamics in Uganda. Parasite Epidemiol Control. 2018;3(3):e00070. https://doi.org/10.1016/j.parepi.2018.e00070.
- Bennett A, Yukich J, Miller JM, Keating J, Moonga H, Hamainza B, et al. The relative contribution of climate variability and vector control coverage to changes in malaria parasite prevalence in Zambia 2006–2012. Parasites Vectors. 2016;9(1):431. https://doi.org/10.1186/s13071-016-1693-0.
- Gemperli A, Sogoba N, Fondjo E, Mabaso M, Bagayoko M, Briët OJT, et al. Mapping malaria transmission in West and central Africa. Trop Med Int

- Health. 2006;11(7):1032–46. https://doi.org/10.1111/j.1365-3156.2006.01640. x.
- Gething PW, Casey DC, Weiss DJ, Bisanzio D, Bhatt S, Cameron E, et al. Mapping plasmodium falciparum mortality in Africa between 1990 and 2015. N Engl J Med. 2016;375(25):2435–45. https://doi.org/10.1056/NEJMoa1606701.
- Kang SY, Battle KE, Gibson HS, Ratsimbasoa A, Randrianarivelojosia M, Ramboarina S, et al. Spatio-temporal mapping of madagascar's malaria indicator survey results to assess plasmodium falciparum endemicity trends between 2011 and 2016. BMC Med. 2018;16(1):71. https://doi.org/10.1186/s12916-01 8-1060-4.
- Kleinschmidt I, Bagayoko M, Clarke G, Craig M, Le Sueur D. A spatial statistical approach to malaria mapping. Int J Epidemiol. 2000;29(2):355–61. https://doi. org/10.1093/ije/29.2.355.
- Blanford Jl. Managing vector-borne diseases in a geoAl-enabled society.
 Malaria as an example. Acta Trop. 2024;107406. https://doi.org/10.1016/j.actatropica.2024.107406.
- Sturrock HJW, Bennett AF, Midekisa A, Gosling RD, Gething PW, Greenhouse B. Mapping malaria risk in low transmission settings: challenges and opportunities. Trends Parasitol. 2016;32(8):635–45. https://doi.org/10.1016/j.pt.2016.0 5.001
- Alegana VA, Okiro EA, Snow RW. Routine data for malaria morbidity estimation in africa: challenges and prospects. BMC Med. 2020;18(1):121. https://doi.org/10.1186/s12916-020-01593-y.
- Ozodiegwu ID, Ambrose M, Battle KE, Bever C, Diallo O, Galatas B, et al. Beyond National indicators: adapting the demographic and health surveys' sampling strategies and questions to better inform subnational malaria intervention policy. Malar J. 2021;20(1):122. https://doi.org/10.1186/s12936-0 21-0346-w
- Gutman JR, Thwing J, Mwesigwa J, McElroy PD, Robertson M. Routine healthcare Facility—and antenatal Care—Based malaria surveillance: challenges and opportunities. Am J Trop Med Hyg. 2023;108(2 Suppl):4–7. https://doi.org/10. 4269/aitmh.22-0182.
- Dlamini SN, Beloconi A, Mabaso S, Vounatsou P, Impouma B, Fall IS. Review of remotely sensed data products for disease mapping and epidemiology. Remote Sens Appl: Soc Environ. 2019;14:108–18. https://doi.org/10.1016/j.rsa se.2019.02.005.
- Aheto JMK. Mapping under-five child malaria risk that accounts for environmental and Climatic factors to aid malaria preventive and control efforts in ghana: bayesian geospatial and interactive web-based mapping methods. Malar J. 2022;21(1):384. https://doi.org/10.1186/s12936-022-04409-x.
- Georganos S, Brousse O, Dujardin S, Linard C, Casey D, Milliones M, et al. Modelling and mapping the intra-urban Spatial distribution of plasmodium falciparum parasite rate using very-high-resolution satellite derived indicators. Int J Health Geogr. 2020;19(1):38. https://doi.org/10.1186/s12942-020-00 232-2.
- Pesaresi M, Huadong G, Blaes X, Ehrlich D, Ferri S, Gueguen L, et al. A global human settlement layer from optical HR/VHR RS data: concept and first results. 2013;6(5):2102–131. https://doi.org/10.1109/JSTARS.2013.2271445.
- Brown CF, Brumby SP, Guzder-Williams B, Birch T, Hyde SB, Mazzariello J, et al. Dynamic world, near real-time global 10 m land use land cover mapping. Sci Data. 2022;9(1):251. https://doi.org/10.1038/s41597-022-01307-4.
- Ebhuoma O, Gebreslasie M. Remote Sensing-Driven climatic/environmental variables for modelling malaria transmission in Sub-Saharan Africa. Int J Environ Res Public Health. 2016;13(6):E584. https://doi.org/10.3390/ijerph130 60584
- 65. PNLP. Bulletin Epidemiologique annuel 2022 du Paludisme au Sénégal. 2022.
- World Health Organization. Global technical strategy for malaria 2016–2030.
 Geneva: World Health Organization; 2015. https://iris.who.int/handle/10665/176712
- 67. Giardina F, Kasasa S, Sié A, Utzinger J, Tanner M, Vounatsou P. Effects of vector-control interventions on changes in risk of malaria parasitaemia in sub-Saharan africa: a spatial and temporal analysis. Lancet Global Health. 2014;2(10):e601–15. https://doi.org/10.1016/S2214-109X(14)70300-6.
- 68. Giardina F, Gosoniu L, Konate L, Diouf MB, Perry R, Gaye O, et al. Estimating the burden of malaria in senegal: bayesian zero-inflated binomial geostatistical modeling of the MIS 2008 data. PLoS ONE. 2012;7(3):e32625. https://doi.org/10.1371/journal.pone.0032625.
- Lucas TCD, Nandi AK, Keddie SH, Chestnutt EG, Howes RE, Rumisha SF, et al. Improving disaggregation models of malaria incidence by ensembling non-linear models of prevalence. Spat Spatio-temporal Epidemiol. 2022;41:100357. https://doi.org/10.1016/j.sste.2020.100357.

- Lucas TCD, Nandi AK, Chestnutt EG, Twohig KA, Keddie SH, Collins EL, et al. Mapping malaria by sharing Spatial information between incidence and prevalence data sets. J R Stat Soc Ser C: Appl Stat. 2021;70(3):733–49. https://doi.org/10.1111/rssc.12484.
- Morlighem C. Integrating vulnerability and hazard in malaria risk mapping. Database: Figshare. 2025. https://doi.org/10.6084/m9.figshare.29189567.v1.
- Cissé B, Ba EH, Sokhna C, NDiaye JL, Gomis JF, Dial Y, et al. Effectiveness of seasonal malaria chemoprevention in children under ten years of age in senegal: a stepped-wedge cluster-randomised trial. PLoS Med. 2016;13(11):e1002175. https://doi.org/10.1371/journal.pmed.1002175.
- Sy O, Niang EHA, Ndiaye M, Konaté L, Diallo A, Ba ECC, et al. Entomological impact of indoor residual spraying with pirimiphos-methyl: a pilot study in an area of low malaria transmission in Senegal. Malar J. 2018;17(1):64. https://doi. org/10.1186/s12936-018-2212-x.
- Croft TN, Marshall AMJ, Allen CK. Guide to DHS Statistics DHS-7. Rockville. Maryland, USA: ICF; 2018. https://www.dhsprogram.com/pubs/pdf/DHSG1/Guide_to_DHS_Statistics_DHS-7_v2.pdf.
- 75. Corsi D, Neuman M, Finlay J, Subramanian S. Demographic and health surveys: a profile. Int J Epidemiol. 2012;41(6):1602–13. https://doi.org/10.1093/ije/dys184.
- Azikiwe C, Ifezulike C, Siminialayi I, Amazu L, Enye J, Nwakwunite O. A comparative laboratory diagnosis of malaria: microscopy versus rapid diagnostic test kits. Asian Pac J Trop Biomed. 2012;2(4):307–10. https://doi.org/10.1016/S 2221-1691(12)60029-X.
- MEASURE Evaluation, The Demographic and Health Surveys Program, President's Malaria Initiative, Roll Back Malaria Partnership, United Nations Children's Fund, World Health Organization. Household Survey Indicators for Malaria Control. 2018. https://www.malariasurveys.org/documents/Household%20Survey%20Indicators%20for%20Malaria%20Control_FINAL.pdf.
- Burgert CR, Colston J, Roy T, Zachary B. Geographic displacement procedure and georeferenced data release policy for the Demographic and Health Surveys. DHS Spatial Analysis Reports No. 7. Calverton, Maryland, USA: ICF International; 2013. https://dhsprogram.com/pubs/pdf/SAR7/SAR7.pdf
- Gething P, Tatem A, Bird T, Burgert-Brucker CR. Creating Spatial Interpolation Surfaces with DHS Data. DHS Spatial Analysis Reports No. 11. Rockville, Maryland, USA: ICF International; 2015. https://dhsprogram.com/pubs/pdf/SAR11/SAR11 pdf
- 80. Georganos S, Gadiaga AN, Linard C, Grippa T, Vanhuysse S, Mboga N, et al. Modelling the wealth index of demographic and health surveys within cities using very High-Resolution remotely sensed information. Remote Sens. 2019;11(21):2543. https://doi.org/10.3390/rs11212543.
- Morlighem C, Chaiban C, Georganos S, Brousse O, Van Lipzig NPM, Wolff E, et al. Spatial optimization methods for malaria risk mapping in Sub-Saharan African cities using demographic and health surveys. GeoHealth. 2023;7(10):e2023GH000787. https://doi.org/10.1029/2023GH000787.
- Bosco C, Alegana V, Bird T, Pezzulo C, Bengtsson L, Sorichetta A, et al. Exploring the high-resolution mapping of gender-disaggregated development indicators. J R Soc Interface. 2017;14(129):20160825. https://doi.org/10.1098/rsif.2016.0825.
- ANSD, [Sénégal] ICF, Sénégal. Enquête démographique et de Santé continue (EDS-Continue 2017). Rockville. Maryland, USA: ANSD and ICF; 2018. https://www.ansd.sn/sites/default/files/2022-11/Rapport%20Final%20EDS%202017_0.pdf
- ANSD, [Sénégal] ICF, Sénégal. Enquête Sur les indicateurs du paludisme (EIPS) 2020–2021. Maryland, USA: ANSD and ICF. Rockville; 2022. https://dhsprogram.com/pubs/pdf/MIS38/MIS38.pdf.
- Karger DN, Conrad O, Böhner J, Kawohl T, Kreft H, Soria-Auza RW, et al. Climatologies at high resolution for the earth's land surface areas. Sci Data. 2017;4(1):170122. https://doi.org/10.1038/sdata.2017.122.
- Wan Z, Hook S, Hulley GMODIS. Terra land surface temperature/emissivity daily L3 global 1km SIN grid V061 [dataset]. NASA EOSDIS Land Processes DAAC; 2021. https://doi.org/10.5067/MODIS/MOD11A1.061
- 87. Wan Z, Hook S, Hulley GMODIS. Aqua land surface temperature/emissivity daily L3 global 1km SIN grid V061 [dataset]. NASA EOSDIS Land Processes DAAC; 2021. https://doi.org/10.5067/MODIS/MYD11A1.061
- Simonetti D, Pimple U, Langner A, Marelli A. Pan-tropical Sentinel-2 cloud-free annual composite datasets. Data Brief. 2021;39:107488. https://doi.org/10.101 6/j.dib.2021.107488.
- Marconcini M, Metz-Marconcini A, Üreyen S, Palacios-Lopez D, Hanke W, Bachofer F, et al. Outlining where humans live, the world settlement footprint 2015. Sci Data. 2020;7(1):242. https://doi.org/10.1038/s41597-020-00580-5.

- Pesaresi M, Politis P. GHS-BUILT-S, R2023A GHS built-up surface grid, derived from Sentinel2 composite and Landsat, multitemporal (1975–2030) [dataset]. European Commission, Joint Research Centre (JRC). 2023. https://doi.org/10. 2905/9F06F36F-4B11-47EC-ABB0-4F8B7B1D72EA
- 91. Pesaresi M, Politis P. GHS-BUILT-C, R2023A GHS settlement characteristics, derived from Sentinel2 composite (2018) and other GHS R2023A data [data-set]. Eur Comm Joint Res Centre (JRC). 2023. https://doi.org/10.2905/3C60DD F6-0586-4190-854B-F6AA0EDC2A30.
- Elvidge CD, Zhizhin M, Ghosh T, Hsu FC, Taneja J. Annual time series of global VIIRS nighttime lights derived from monthly averages: 2012 to 2019. Remote Sens. 2021;13(5):922. https://doi.org/10.3390/rs13050922.
- 93. Farr TG, Rosen PA, Caro E, Crippen R, Duren R, Hensley S, et al. The shuttle radar topography mission. Rev Geophys. 2007;45(2):RG2004. https://doi.org/10.1029/2005RG000183.
- 94. WorldPop (www.worldpop.org School of Geography and Environmental Science, University of Southampton; Department of Geography and Geosciences, University of Louisville; Departement de Geographie, Universite de Namur) and Center for International Earth Science Information Network (CIE-SIN), Columbia University. Global High Resolution Population Denominators Project - Funded by The Bill and Melinda Gates Foundation (OPP1134076) [dataset]. 2018. https://doi.org/10.5258/SOTON/WP00645.
- Robinson TP, Wint GRW, Conchedda G, Boeckel TPV, Ercoli V, Palamara E, et al. Mapping the global distribution of livestock. PLoS One. 2014;9(5):e96084. htt ps://doi.org/10.1371/journal.pone.0096084.
- WorldPop (www.worldpop.org School of Geography and Environmental Science, University of Southampton). Senegal 1km pregnancies. Version 2.0 2015 estimates of numbers of pregnancies per grid square, with national totals adjusted to match national estimates on numbers of pregnancies made by the Guttmacher Institute (https://www.guttmacher.org) [dataset]. 2017. https://doi.org/10.5258/SOTON/WP00448.
- WorldPop (www.worldpop.org School of Geography and Environmental Science, University of Southampton; Department of Geography and Geosciences, University of Louisville; Departement de Geographie, Universite de Namur) and Center for International Earth Science Information Network (CIE-SIN), Columbia University. Global High Resolution Population Denominators Project - Funded by The Bill and Melinda Gates Foundation (OPP1134076) [dataset]. 2018. https://doi.org/10.5258/SOTON/WP00646
- Müller-Crepon C, Hunziker P. New Spatial data on ethnicity: introducing SIDE. J Peace Res. 2018;55(5):687–98. https://doi.org/10.1177/0022343318764254.
- OpenStreetMap contributors. OpenStreetMap [dataset]. Available under the open database licence from: openstreetmap.org. Cambridge. UK: Open-StreetMap Foundation; 2025. https://www.openstreetmap.org/.
- 100. Weiss DJ, Nelson A, Gibson HS, Temperley W, Peedell S, Lieber A, et al. A global map of travel time to cities to assess inequalities in accessibility in 2015. Nature. 2018;553(7688):333–6. https://doi.org/10.1038/nature25181.
- Weiss DJ, Nelson A, Vargas-Ruiz CA, Gligorić K, Bavadekar S, Gabrilovich E, et al. Global maps of travel time to healthcare facilities. Nat Med. 2020;26(12):1835–8. https://doi.org/10.1038/s41591-020-1059-1.
- Craig MH, Snow RW, le Sueur D. A climate-based distribution model of malaria transmission in sub-Saharan Africa. Parasitol Today (Personal Ed). 1999;15(3):105–11. https://doi.org/10.1016/s0169-4758(99)01396-4.
- Akinbobola A, Omotosho JB. Predicting malaria occurrence in Southwest and North central Nigeria using meteorological parameters. Int J Biometeorol. 2013;57(5):721–8. https://doi.org/10.1007/s00484-012-0599-6.
- 104. le Sueur D, Sharp BL. The breeding requirements of three members of the Anopheles Gambiae Giles complex (Diptera: Culicidae) in the endemic malaria area of natal, South Africa. Bull Entomol Res. 1988;78(4):549–60. https: //doi.org/10.1017/S0007485300015418.
- 105. Jepson WF, Moutia A, Courtois C. The malaria problem in mauritius: the bionomics of Mauritian anophelines. Bull Entomol Res. 1947;38(1):177–208. h ttps://doi.org/10.1017/S0007485300030273.
- 106. Kabaria CW, Molteni F, Mandike R, Chacky F, Noor AM, Snow RW, et al. Mapping intra-urban malaria risk using high resolution satellite imagery: a case study of Dar Es Salaam. Int J Health Geogr. 2016;15(1):26. https://doi.org/10.1 186/s12942-016-0051-y.
- 107. Morlighem C, Chaiban C, Georganos S, Brousse O, Van de Walle J, van Lipzig NPM, et al. The multi-satellite environmental and socioeconomic predictors of Vector-Borne diseases in African cities: malaria as an example. Remote Sens. 2022;14(21):5381. https://doi.org/10.3390/rs14215381.
- Tatem AJ, Gething PW, Smith DL, Hay SI. Urbanization and the global malaria recession. Malar J. 2013;12(1):133. https://doi.org/10.1186/1475-2875-12-133.

- 109. Atieli HE, Zhou G, Lee MC, Kweka EJ, Afrane Y, Mwanzo I, et al. Topography as a modifier of breeding habitats and concurrent vulnerability to malaria risk in the Western Kenya highlands. Parasites Vectors. 2011;4(1):241. https://doi.org/ 10.1186/1756-3305-4-241.
- Nmor JC, Sunahara T, Goto K, Futami K, Sonye G, Akweywa P, et al. Topographic models for predicting malaria vector breeding habitats: potential tools for vector control managers. Parasites Vectors. 2013;6(1):14. https://doi.org/10.1186/1756-3305-6-14.
- 111. Morgan CE, Topazian HM, Brandt K, Mitchell C, Kashamuka MM, Muwonga J, et al. Association between domesticated animal ownership and plasmodium falciparum parasite prevalence in the Democratic Republic of the congo: a National cross-sectional study. Lancet Microbe. 2023;4(7):e516–23. https://doi.org/10.1016/S2666-5247(23)00109-X.
- 112. Yang D, He Y, Wu B, Deng Y, Li M, Yang Q, et al. Drinking water and sanitation conditions are associated with the risk of malaria among children under five years old in sub-Saharan africa: a logistic regression model analysis of National survey data. J Adv Res. 2020;21:1–13. https://doi.org/10.1016/j.jare.2019.09.001.
- 113. Oldenburg CE, Guerin PJ, Berthé F, Grais RF, Isanaka S. Malaria and nutritional status among children with severe acute malnutrition in niger: a prospective cohort study. Clin Infect Dis. 2018;67(7):1027–34. https://doi.org/10.1093/cid/ civ207.
- Protopopoff N, Bortel WV, Speybroeck N, Geertruyden JPV, Baza D, D'Alessandro U, et al. Ranking malaria risk factors to guide malaria control efforts in African highlands. PLoS One. 2009;4(11):e8022. https://doi.org/10.13 71/journal.pone.0008022.
- 115. Sarfo JO, Amoadu M, Kordorwu PY, Adams AK, Gyan TB, Osman AG, et al. Malaria amongst children under five in sub-Saharan africa: a scoping review of prevalence, risk factors and preventive interventions. Eur J Med Res. 2023;28(1):80. https://doi.org/10.1186/s40001-023-01046-1.
- White NJ. Anaemia and malaria. Malar J. 2018;17(1):371. https://doi.org/10.11 86/s12936-018-2509-9.
- 117. Bates I, Fenton C, Gruber J, Lalloo D, Lara AM, Squire SB, et al. Vulnerability to malaria, tuberculosis, and HIV/AIDS infection and disease. Part II: determinants operating at environmental and institutional level. Lancet Infect Dis. 2004;4(6):368–75. https://doi.org/10.1016/S1473-3099(04)01047-3.
- 118. DHS Spatial Interpolation Working Group. Spatial Interpolation with Demographic and Health Survey Data: Key Considerations. Rockville, Maryland, USA: ICF International; 2014. https://dhsprogram.com/pubs/pdf/SAR9/SAR9.pdf. (DHS Spatial Analysis Reports No. 9).
- Utazi CE, Thorley J, Alegana VA, Ferrari MJ, Takahashi S, Metcalf CJE, et al. High resolution age-structured mapping of childhood vaccination coverage in low and middle income countries. Vaccine. 2018;36(12):1583–91. https://doi.org/ 10.1016/j.vaccine.2018.02.020.
- Perez-Heydrich C, Warren JL, Burgert CR, Emch ME. Guidelines on the use of DHS GPS data. Maryland, USA: ICF International, Calverton; 2013. https://dhsprogram.com/pubs/pdf/SAR8/SAR8.pdf. (DHS Spatial Analysis Reports No. 8.).
- 121. Brousse O, Georganos S, Demuzere M, Dujardin S, Lennert M, Linard C, et al. Can we use local climate zones for predicting malaria prevalence across sub-Saharan African cities? Environ Res Lett. 2020;15(12):124051. https://doi.org/10.1088/1748-9326/abc996.
- 122. Krainski ET, Gómez-Rubio V, Bakka H, Lenzi A, Castro-Camilo D, Simpson D, et al. Advanced Spatial modeling with stochastic partial differential equations using R and INLA. Boca Raton, FL: Chapman & Hall/CRC; 2019.
- 123. Riedel N, Vounatsou P, Miller JM, Gosoniu L, Chizema-Kawesha E, Mukonka V, et al. Geographical patterns and predictors of malaria risk in zambia: bayesian geostatistical modelling of the 2006 Zambia National malaria indicator survey (ZMIS). Malar J. 2010;9(1):37. https://doi.org/10.1186/1475-2875-9-37.
- Adigun AB, Gajere EN, Oresanya O, Vounatsou P. Malaria risk in nigeria: bayesian Geostatistical modelling of 2010 malaria indicator survey data. Malar J. 2015;14(1):156. https://doi.org/10.1186/s12936-015-0683-6.
- 125. Ibeji JU, Mwambi H, Iddrisu AK. Bayesian spatio-temporal modelling and mapping of malaria and anaemia among children between 0 and 59 months in Nigeria. Malar J. 2022;21(1):311. https://doi.org/10.1186/s12936-022-0431
- 126. Rue H, Martino S, Chopin N. Approximate bayesian inference for latent Gaussian models by using integrated nested Laplace approximations. J R Stat Soc: Ser B (Statistical Methodology). 2009;71(2):319–92. https://doi.org/10.1111/j.1467-9868.2008.00700.x.
- 127. Lindgren F, Rue H, Lindström J. An explicit link between Gaussian fields and Gaussian Markov random fields: the stochastic partial differential equation

- approach. J R Stat Soc Ser B: Stat Methodol. 2011;73(4):423–98. https://doi.org/10.1111/j.1467-9868.2011.00777.x.
- 128. Gomez-Rubio V. Bayesian inference with INLA. New York: Chapman and Hall/CRC. 2020;330. https://doi.org/10.1201/9781315175584p.
- 129. Morlighem C, Nnanatu CC, Visée C, Fall A, Linard C. Spatial interpolation of health and demographic variables: predicting malaria indicators with and without covariates. PLoS One. 2025;20(5):e0322819. https://doi.org/10.1371/j ournal.pone.0322819.
- Spiegelhalter DJ, Best NG, Carlin BP, Van Der Linde A. Bayesian measures of model complexity and fit. J Royal Stat Soc Ser B: Stat Methodol. 2002;64(4):583–639. https://doi.org/10.1111/1467-9868.00353.
- James G, Witten D, Hastie T, Tibshirani R. An introduction to statistical learning: with applications. Volume 6. New York: Springer; 2013. https://doi.org/10.1007/978-1-0716-1418-1.
- Tairou F, Diallo A, Sy O, Kone A, Manga IA, Sylla K, et al. Malaria-associated risk factors among adolescents living in areas with persistent transmission in senegal: a case–control study. Malar J. 2022;21(1):193. https://doi.org/10.1186 /s12936-022-04212-8.
- Gosoniu L, Msengwa A, Lengeler C, Vounatsou P. Spatially explicit burden estimates of malaria in Tanzania: Bayesian geostatistical modeling of the malaria indicator survey data. PLOS ONE. 2012;7(5):e23966. https://doi.org/10. 1371/journal.pone.0023966.
- Ejigu BA. Geostatistical analysis and mapping of malaria risk in children of Mozambique. PLOS ONE. 2020;15(11):e0241680. https://doi.org/10.1371/journal.pone.0241680
- 135. Aheto JMK, Duah HO, Agbadi P, Nakua EK. A predictive model, and predictors of under-five child malaria prevalence in ghana: how do LASSO, ridge and elastic net regression approaches compare? Prev Med Rep. 2021;23:101475. h ttps://doi.org/10.1016/j.pmedr.2021.101475.
- 136. Traub-Merz R, Öhm M. Accès aux services de santé: Une Demande Clé de La main-d'œuvre Informelle En afrique—Résultats d'enquêtes nationales représentatives En afrique subsaharienne. Berlin, Allemagne: Friedrich-Ebert-Stiftung: 2021.
- Asori M, Musah A, Odei J, Morgan AK, Zurikanen I. Spatio-temporal assessment of hotspots and seasonally adjusted environmental risk factors of malaria prevalence. Appl Geogr. 2023;160:103104. https://doi.org/10.1016/j.a pgeog.2023.103104.
- 138. Mitchell CL, Ngasala B, Janko MM, Chacky F, Edwards JK, Pence BW, et al. Evaluating malaria prevalence and land cover across varying transmission intensity in Tanzania using a cross-sectional survey of school-aged children. Malar J. 2022;21(1):80. https://doi.org/10.1186/s12936-022-04107-8.
- 139. Vanhuysse S, Diédhiou SM, Grippa T, Georganos S, Konaté L, Niang EHA, et al. Fine-scale mapping of urban malaria exposure under data scarcity: an approach centred on vector ecology. Malar J. 2023;22(1):113. https://doi.org/ 10.1186/s12936-023-04527-0.
- 140. Birane C, Niang DA, Louis NJ, André DJ, Christopher B, Quensière J et al. Facteurs de risque environnementaux de La persistance du paludisme Dans La banlieue de Dakar (Guédiawaye– Pikine). Int J Innov Appl Stud. 2016;15(2).
- 141. Machault V, Vignolles C, Pagès F, Gadiaga L, Gaye A, Sokhna C, et al. Spatial heterogeneity and Temporal evolution of malaria transmission risk in dakar, senegal, according to remotely sensed environmental data. Malar J. 2010;9(1):252. https://doi.org/10.1186/1475-2875-9-252.
- Diop A, Ndiaye F, Sturm-Ramirez K, Konate L, Senghor M, Diouf EH, et al. Urban malaria vector bionomics and human sleeping behavior in three cities in Senegal. Parasites Vectors. 2023;16:331. https://doi.org/10.1186/s13071-02 3-05032-9
- 143. Ndiaye F, Diop A, Chabi J, Sturm-Ramirez K, Senghor M, Diouf EH, et al. Distribution and dynamics of Anopheles Gambiae s.l. Larval habitats in three Senegalese cities with high urban malaria incidence. PLoS One. 2024;19(5):e0303473. https://doi.org/10.1371/journal.pone.0303473.
- 144. PNLP. Bulletin Epidemiologique annuel 2017 du Paludisme au Sénégal. 2018. https://africacheck.org/sites/default/files/sources/Senegal-paludisme-bulletin-annuel-2017-PNLP.pdf.
- 145. Sokhna C, Mboup BM, Sow PG, Camara G, Dieng M, Sylla M, et al. Communicable and non-communicable disease risks at the *Grand Magal* of touba: the largest mass gathering in Senegal. Travel Med Infect Dis. 2017;19:56–60. https://doi.org/10.1016/itmaid.2017.08.005.
- 146. Sokhna C, Goumballa N, Hoang VT, Mboup BM, Dieng M, Sylla AB, et al. Senegal's grand Magal of touba: syndromic surveillance during the 2016 mass gathering. Am J Trop Med Hyg. 2020;102(2):476–82. https://doi.org/10.4269/ajtmh.19-0240.

- Ndione B. Migration au Sénégal. Profil national 2018. Dakar, Sénégal: ANSD, IOM; 2018. https://publications.iom.int/system/files/pdf/mp_senegal_2018_fr.pdf.
- Erhabor O, Azuonwu O, Frank-Peterside N. Malaria parasitaemia among long distance truck drivers in the Niger delta of Nigeria. Afr Health Sci. 2012;12(2):98–103. https://doi.org/10.4314/ahs.v12i2.4.
- Pagel J. A natural resource curse: the unintended effects of gold mining on malaria. Ecol Econ. 2025;230:108469. https://doi.org/10.1016/j.ecolecon.2024. 108469.
- Tatem AJ, Smith DL. International population movements and regional plasmodium falciparum malaria elimination strategies. Proc Natl Acad Sci. 2010;107(27):12222–7. https://doi.org/10.1073/pnas.1002971107.
- Williams NE, Thomas TA, Dunbar M, Eagle N, Dobra A. Measures of human mobility using mobile phone records enhanced with GIS data. PLOS ONE. 2015;10(7):e0133630. https://doi.org/10.1371/journal.pone.0133630.
- Lindblade KA, Steinhardt, Laura S, Aaron, Kachur S, Patrick, Slutsker L. The silent threat: asymptomatic parasitemia and malaria transmission. Expert Rev Anti-infect Therapy. 2013;11(6):623–39. https://doi.org/10.1586/eri.13.45.
- 153. Epstein A, Namuganga JF, Nabende I, Kamya EV, Kamya MR, Dorsey G, et al. Mapping malaria incidence using routine health facility surveillance data in Uganda. BMJ Global Health. 2023;8(5):e011137. https://doi.org/10.1136/bmjg h-2022-011137.
- 154. Danwang C, Khalil É, Achu D, Ateba M, Abomabo M, Souopgui J, et al. Fine scale analysis of malaria incidence in under-5: hierarchical bayesian spatiotemporal modelling of routinely collected malaria data between 2012–2018 in Cameroon. Sci Rep. 2021;11. https://doi.org/10.1038/s41598-021-90997-8.
- 155. Lubinda J, Bi Y, Haque U, Lubinda M, Hamainza B, Moore AJ. Spatio-temporal monitoring of health facility-level malaria trends in Zambia and adaptive scaling for operational intervention. Commun Med. 2022;2(1):1–12. https://doi.or a/10.1038/s43856-022-00144-1.
- Arambepola R, Keddie SH, Collins EL, Twohig KA, Amratia P, Bertozzi-Villa A, et al. Spatiotemporal mapping of malaria prevalence in Madagascar using routine surveillance and health survey data. Sci Rep. 2020;10(1):18129. https://doi.org/10.1038/s41598-020-75189-0.
- 157. Kang SY, Amratia P, Dunn J, Vilay P, Connell M, Symons T, et al. Fine-scale maps of malaria incidence to inform risk stratification in Laos. Malar J. 2024;23(1):196. https://doi.org/10.1186/s12936-024-05007-9.
- 158. Cameron E, Young AJ, Twohig KA, Pothin E, Bhavnani D, Dismer A, et al. Mapping the endemicity and seasonality of clinical malaria for intervention targeting in Haiti using routine case data. eLife. 2021;10:e62122. https://doi.org/10.7554/eLife.62122.
- 159. Dlamini SN, Fall IS, Mabaso SD. Bayesian Geostatistical modeling to assess malaria seasonality and monthly incidence risk in Eswatini. J Epidemiol Global Health. 2022;12(3):340–61. https://doi.org/10.1007/s44197-022-0005 4-4
- Elagali A, Ahmed A, Makki N, Ismail H, Ajak M, Alene KA, et al. Spatiotemporal mapping of malaria incidence in Sudan using routine surveillance data. Sci Rep. 2022;12(1):14114. https://doi.org/10.1038/s41598-022-16706-1.
- 161. Golding N, Burstein R, Longbottom J, Browne AJ, Fullman N, Osgood-Zimmerman A, et al. Mapping under-5 and neonatal mortality in africa, 2000–15: a baseline analysis for the sustainable development goals. Lancet. 2017;390(10108):2171–82. https://doi.org/10.1016/S0140-6736(17)31758-0.
- 162. Fornace KM, Senyonjo L, Martin DL, Gwyn S, Schmidt E, Agyemang D, et al. Characterising Spatial patterns of neglected tropical disease transmission using integrated sero-surveillance in Northern Ghana. PLoS Negl Trop Dis. 2022;16(3):e0010227. https://doi.org/10.1371/journal.pntd.0010227.
- 163. Harrison LE, Flegg JA, Tobin R, Lubis IND, Noviyanti R, Grigg MJ, et al. A multi-criteria framework for disease surveillance site selection: case study for plasmodium Knowlesi malaria in Indonesia. Royal Soc Open Sci. 2024;11(1):230641. https://doi.org/10.1098/rsos.230641.
- 164. Zhao C, Wang Y, Tiseo K, Pires J, Criscuolo NG, Van Boeckel TP. Geographically targeted surveillance of livestock could help prioritize intervention against antimicrobial resistance in China. Nat Food. 2021;2(8):596–602. https://doi.org/10.1038/s43016-021-00320-x.
- 165. Blangiardo M, Cameletti M. Spatial and Spatio-temporal bayesian models with R-INLA. Wiley; 2015. https://doi.org/10.1002/9781118950203.

Publisher's note

Springer Nature remains neutral with regard to jurisdictional claims in published maps and institutional affiliations.